Title: Metabolism and Disposition of a Novel Bcl-2 Inhibitor Venetoclax in Humans and Characterization of its Unusual Metabolites

Authors: Hong Liu, Melissa J. Michmerhuizen, Yanbin Lao, Katty Wan, Ahmed Hamed Salem, James Sawicki, Michael Serby, Srirajan Vaidyanathan, Shekman L. Wong, Suresh Agarwal, Martin Dunbar, Jens Sydor, Sonia M. de Morais, Anthony J. Lee

Bioanalysis and Biotransformation, Research & Development, AbbVie, North Chicago, Illinois (H.L., M.J.M., K.W., J.S., M.S., J.S., S.M.M., A.J.L.); Process Chemistry, AbbVie, North Chicago, Illinois (S.V.); Clinical Pharmacology and Pharmacometrics, AbbVie, North Chicago, Illinois (A.H.S., S.L.W., S.A., M.D.); Clinical Pharmacy, Faculty of Pharmacy, Ain Shams University, Cairo, Egypt (A.H.S.); Eli Lilly and Company, Indianapolis, IN (Y.L.)

DMD Fast Forward. Published on December 19, 2016 as DOI: 10.1124/dmd.116.071613
This article has not been copyedited and formatted. The final version may differ from this version.

Running Title: Absorption, metabolism, and excretion of venetoclax in humans.

Corresponding author: Dr. Hong Liu, Bioanalysis and Biotransformation, AbbVie, 1 N. Waukegan Rd., North Chicago, IL 60064. Email: hong.liu@abbvie.com

Number of text pages: 36

Number of tables: 3

Number of figures: 8

Number of reference: 28

Number of words in the Abstract: 250

Number of words in the Introduction: 426

Number of words in the Discussion: 1464

ABBREVIATIONS: AML, acute myeloid leukemia; AUC, area under the curve; Bcl-2, B-cell lymphoma-2; CLL, chronic lymphocytic leukemia; cpm, counts per minute; CYP, cytochrome P450; CID, collision-induced dissociation; DMSO, dimethyl sulfoxide; dpm, disintegrations per minute; DPBS, Dulbecco's phosphate buffered saline; FDA, U.S. Food and Drug Administration; HPLC, high-performance liquid chromatography; (K_2-EDTA), di-potassium ethylenediaminetetraacetate; LLOQ, lower limit of quantitation; LSC, liquid scintillation counting; μCi, microcuries; MTD, maximal tolerated dose; NADHP, nicotinamide adenine dinucleotide phosphate; ppm, parts per million; SLL, small lymphocytic lymphoma; SPE, solid phase extraction

Abstract

Venetoclax (ABT-199) is a Bcl-2 protein inhibitor and is currently in clinical development for the treatment of hematological malignancies. The objective of this study was to characterize the absorption, metabolism, and excretion of venetoclax in humans. Following a single oral dose of of [^{14}C]venetoclax to healthy volunteers, recovery of total radioactive dose was 100%, with feces being the major route of elimination of the administered dose, whereas urinary excretion was minimal (<0.1%). The extent of absorption was estimated to be at least 65%. Venetoclax was primarily cleared by hepatic metabolism (~66% of the administered dose). ~33% of the administered dose was recovered as parent drug and its nitro reduction metabolite M30 (13%) in feces. Biotransformation of venetoclax in human primarily involves enzymatic oxidation on the dimethyl cyclohexenyl moiety, followed by sulfation and/or nitro reduction. Nitro reduction metabolites were likely formed by gut bacteria. Unchanged venetoclax was the major drug-related material in circulation, representing 72.8% of total plasma radioactivity. M27 (oxidation at the 6 position of cyclohexenyl ring followed by cyclization at the α-carbon of piperazine ring) was identified as a major metabolite representing 12% of total drug related material. M27 was primarily formed by CYP3A4. Steady-state plasma concentrations of M27 in human and preclinical species used for safety testing suggested that M27 is a disproportionate human metabolite. M27 is not expected to have clinically relevant on- or off-target pharmacological activities. In summary, the study characterized venetoclax metabolites in circulation and feces and the primary elimination pathway of venetoclax in human.

DMD Fast Forward. Published on December 19, 2016 as DOI: 10.1124/dmd.116.071613
This article has not been copyedited and formatted. The final version may differ from this version.

Introduction

Chronic lymphocytic leukemia (CLL) is the most common form of leukemia in the Western world, representing about 30% of leukemias (Zenz et al., 2010; Jaglowski and Jones, 2011; Shenoy et al., 2011). CLL is an incurable disease of variable clinical course with a significant impact on life-expectancy. Antiapoptotic B-cell lymphoma-2 (Bcl-2) family proteins are important regulators of the intrinsic apoptosis pathway. Constitutively elevated expression of the antiapoptotic protein Bcl-2 renders CLL cells resistant to apoptosis, resulting in the accumulation of long-lived, clonal lymphocytes that characterize the disease (Robertson et al., 1996; Brown and Dunmore, 2007). Therefore, Bcl-2, a protein central to the survival of CLL cells is an attractive target for CLL therapy. Venetoclax (also known as ABT-199 and GDC-0199) is a novel, orally bioavailable Bcl-2 family protein inhibitor that is being developed for the treatment of CLL and other hematological malignancies. Venetoclax selectively binds with high affinity to Bcl-2 (K_i<0.01 nM) and with three orders of magnitude less affinity to other Bcl-2 family protein members (K_i=48 nM for Bcl-X_L, K_i=245 nM for Bcl-w) (Souers et al., 2013). Venetoclax has been studied in multiple clinical trials and has shown efficacy as a single agent and as combination therapy in patients with relapsed CLL or small lymphocytic lymphoma (SLL) and other hematological malignancies (DiNardo et al., 2015; Moreau et al., 2015; Davids et al., 2016; Konopleva et al., 2016; Roberts et al., 2016). The U.S. Food and Drug Administration (FDA) granted three Breakthrough Therapy Designations to venetoclax as a single agent or in combination with other agents for the treatment of CLL or acute myeloid leukemia (AML) and most recently U.S. FDA approved venetoclax tablets for patients with CLL with 17p deletion who have received at least one prior therapy.

Pharmacokinetics of venetoclax has been thoroughly characterized (Roberts et al., 2016; Salem et al., 2016b). In patients with CLL or SLL, venetoclax plasma concentrations peaked at 6 to 8 hours after a single oral dose and the terminal phase elimination half-life was approximately 19 hours. At steady state, venetoclax exposure (maximal level and area under the curve value) was approximately proportional for doses ranging from 150 mg to 800 mg per day. In vitro studies showed that venetoclax is metabolized primarily by CYP 3A4, consistent with observations from drug-drug interaction studies with ketoconazole, posaconazole, and rifampin (Agarwal et al., 2016a; Agarwal et al., 2016b).

The objective of this study was to investigate the absorption, metabolism, and elimination of venetoclax in healthy female volunteers who received a single oral dose of 200 mg venetoclax containing [^{14}C]venetoclax (100 μCi/subject).

Materials and Methods

Drugs and Reagents

Venetoclax, 4-(4-{[2-(4-chlorophenyl)-4,4-dimethylcyclohex-1-en-1-yl]methyl}piperazin-1-yl)-*N*-({3-nitro-4-[(tetrahydro-2H-pyran-4-ylmethyl)amino]phenyl}sulfonyl)-2-(1H-pyrrolo[2,3-b]pyridin-5-yloxy)benzamide; M3, 4-[4-[[2-(4-chlorophenyl)-3-hydroxy-4,4-dimethyl-cyclohexen-1-yl]methyl]piperazin-1-yl]-N-[3-nitro-4-(tetrahydropyran-4-ylmethylamino)phenyl]sulfonyl-2-(1H-pyrrolo[2,3-b]pyridin-5-yloxy)benzamide; M5, 4-[4-[[2-(4-chlorophenyl)-6-hydroxy-4,4-dimethyl-cyclohexen-1-yl]methyl]piperazin-1-yl]-*N*-[3-nitro-4-(tetrahydropyran-4-ylmethylamino)phenyl]sulfonyl-2-(1H-pyrrolo[2,3-b]pyridin-5-yloxy)benzamide; M6, 4-[4-[[2-(4-chlorophenyl)-4,4-dimethyl-cyclohexen-1-yl]methyl]-4-oxido-piperazin-4-ium-1-yl]-N-[3-nitro-4-(tetrahydropyran-4-ylmethylamino)phenyl]sulfonyl-2-(1H-pyrrolo[2,3-b]pyridin-5-yloxy)benzamide; M14, 4-[4-[[2-(4-chlorophenyl)-4,4-dimethyl-

DMD Fast Forward. Published on December 19, 2016 as DOI: 10.1124/dmd.116.071613
This article has not been copyedited and formatted. The final version may differ from this version.

cyclohexen-1-yl]methyl]-2-oxo-piperazin-1-yl]-N-[3-nitro-4-(tetrahydropyran-4-ylmethylamino)phenyl]sulfonyl-2-(1H-pyrrolo[2,3-b]pyridin-5-yloxy)benzamide; M27, 4-[(10aR,11aS)-7-(4-chlorophenyl)-9,9-dimethyl-1,3,4,6,8,10,10a,11a-octahydropyrazino[2,1-b][1,3]benzoxazin-2-yl]-*N*-[3-nitro-4-(tetrahydropyran-4-ylmethylamino)phenyl]sulfonyl-2-(1H-pyrrolo[2,3-b]pyridin-5-yloxy). Venetoclax, M3, M5, M6, M14 and M27 reference standards were supplied by Process Chemistry, AbbVie, Inc. (North Chicago, IL) and were used as HPLC and mass spectrometric standards. [^{14}C]venetoclax was synthesized in 5 steps starting from [^{14}C]carbonyl labeled 2, 4-difluoro methyl benzoate. Purification of the compound by crystallization provided >99% radiochemical purity by HPLC. All high performance liquid chromatography (HPLC)-grade solvents used for liquid chromatography-tandem mass spectrometry (LC-MS/MS) analysis were purchased from Sigma-Aldrich (St. Louis, MO). The scintillation fluids used for radioanalysis were purchased from PerkinElmer (Waltham, MA)

Clinical Study

The clinical study was conducted at Covance Laboratories Inc., in conjunction with the Covance Clinical Research Unit (Madison, WI). This was a Phase 1, single radiolabeled dose, open-label, single center, mass balance study. The study was conducted in accordance with Good Clinical Practice guidelines and ethical principles that have their origin in the Declaration of Helsinki. The study protocol was approved by the Midlands Independent Review Board (Overland Park, KS), and all subjects provided written informed consent before any study-related procedures were performed. The radioactive dose of 100 μCi was chosen so that the radiation burden for healthy volunteers remained below the allowable United States FDA whole body exposure limits of 3000 mRem for a single dose of radioactivity. The single dose of 200 mg ABT-199 for this open-label study was selected based on the clinical experience in other studies where doses up to

200 mg were safely administered in healthy volunteers (Agarwal et al., 2016a; Salem et al., 2016a).

A total of four female subjects in general good health, of non-childbearing potential, were selected to participate in the study according to the selection criteria. On the morning of Study Day 1, subjects received a single oral dose of [^{14}C]venetoclax approximately 30 minutes after completion of a moderate-fat breakfast. Food increases venetoclax exposure by 3-5 fold and venetoclax is indicated to be taken with meal to optimize the exposure. Therefore, venetoclax was administered under fed conditions in this study to mimic the clinically relevant conditions (Salem et al., 2016a). The study drug, venetoclax (200 mg active, 100 microcuries (μCi)), was administered orally via syringe as an approximately 4 mL liquid solution (polyoxyl 40 hydrogenated castor oil/polyethylene glycol 400 NF/purified oleic acid NF/USP, 1/1/8, w/w/w), followed by approximately 240 mL of additional water. Subjects were confined to the study site and supervised beginning on Study Day-1 and continuing through 216 hours after dosing and completion of study activities. Subjects were released from the study site at any time after 216 hours post dose, once either of the following conditions was met: 1) greater than 90% of the total radioactivity was recovered, or 2) less than 1% of the radioactive dose was recovered in two consecutive 24-hour collection periods. For all subjects, blood sampling was completed after the sample at 216 hours post-dose since greater than 90% of total radioactivity was recovered. Blood samples were collected by venipuncture into vacutainer collection tubes containing di-potassium ethylenediaminetetraacetate (K_2-EDTA) at the following time points: 0 hour (predose), 0.5, 1, 2, 3, 4, 5, 6, 8, 10, 12, 24, 36, 48, 72, 96, 120, 144, 168, 192 and 216 hours after [^{14}C]venetoclax dosing. Plasma was separated via centrifugation and stored at –70°C.

Urine samples were collected predose and over the following intervals: 0 to 12, 12 to 24, 24 to 48, 48 to 72, 72 to 96, 96 to 120, 120 to 144, 144 to 168, 168 to 192 and 192 to 216 hours after [^{14}C]venetoclax dosing. Urine samples were collected into a collection jar containing approximately 3 mL of Tween 20 to minimize non-specific binding with the container. Aliquots of the urine were frozen and maintained at –20°C prior to total radioactivity determination and metabolite profile and identification.

Fecal samples were collected predose (upon check-in before dosing) and over the following intervals after dosing: 0 to 24, 24 to 48, 48 to 72, 72 to 96, 96 to 120, 120 to 144, 144 to 168, 168 to 192 and 192 to 216 hours after dosing of [^{14}C]venetoclax on Study Day 1. All fecal samples collected during a collection interval were kept frozen at -20 °C prior to total radioactivity analysis and metabolite profile and identification.

Total Radioactivity Measurement by Liquid Scintillation Counting (LSC)

All sample combustion was performed using a Model 307 Sample Oxidizer (Packard Instrument Company) and the resulting $^{14}CO_2$ was trapped in Carbo-Sorb and mixed with Perma Fluor. Oxidation efficiency was evaluated on each day of sample combustion by analyzing a commercial radiolabeled standard both directly in scintillation cocktail and by oxidation. Acceptance criteria were defined as combustion recoveries of 95 to 105%. Ecolite (+) scintillation cocktail was used for samples analyzed directly. All samples were analyzed for radioactivity in Model 2900TR or 2940TR liquid scintillation counters (Packard Instrument Company) for at least 5 minutes or 100,000 counts. Each sample was homogenized or mixed before radioanalysis (unless the entire sample was used for analysis). All samples were analyzed in duplicate if the sample size allowed. If results from sample replicates (calculated as ^{14}C disintegrations per minute (dpm)/g sample) differed by more than 10% from the mean value and

sample aliquots had radioactivity greater than 200 dpm, the sample was rehomogenized or remixed and reanalyzed (if the sample size permitted). Scintillation counting data (counts per minute (cpm)) were automatically corrected for counting efficiency using the external standardization technique and an instrument-stored quench curve generated from a series of sealed quenched standards.

Blood samples were mixed and duplicate weighed aliquots (approximately 0.2 g) were combusted and analyzed by LSC. The representative lower limit of quantitation (LLOQ) for blood was 96.6 ng equivalents/g. Plasma samples were mixed and duplicate weighed aliquots (approximately 0.2 g) were analyzed directly by LSC. The representative LLOQ for plasma was 82.5 ng equivalents/g. The urine samples were mixed and duplicate weighed aliquots (approximately 0.2 g) were analyzed directly by LSC. The representative LLOQ for urine was 87.2 ng equivalents/g. Fecal samples were combined by subject at 24-hour intervals and the weight of each combined sample was recorded. A weighed amount of ethanol/water (7/3, v/v) was added and the sample was mixed. The sample was homogenized using a probe-type homogenizer. Duplicate weighed aliquots (approximately 0.2 g) were combusted and analyzed by LSC. The representative LLOQ for feces was 377 ng equivalents/g.

Sample Preparation for Metabolite Profiling

Plasma samples were thawed at room temperature and pooled across subjects per time point and AUC pooled utilizing the Hamilton method (Hamilton et al., 1981). Plasma samples were processed using a solid phase extraction (SPE) method. In brief, pooled plasma (5 mL/column) was loaded onto a Water Oasis HLB column cartridge (6 g/35 cc, Waters Corporation, Milford, MA) that was pre-activated with 20 mL of methanol followed by 20 mL of water. After the sample was loaded, the column was washed with 25 mL of water. Analytes were eluted with 25

mL of methanol, followed by 25 mL of acetonitrile twice. Organic fractions were combined and concentrated to approximately 200 µL utilizing a combination of speed vac (Eppendorf, Hamburg, Germany) and a stream of nitrogen in glass tubes. Samples were diluted with 200 µL of DMSO and 100 µL of acetonitrile/water (1/1, v/v) before HPLC-MS-radioflow analysis. An aliquot of the reconstituted sample was subjected to LSC analysis to determine the total radioactivity recovery. The reconstituted sample (~200 µL) was manually injected for HPLC-MS-radioflow analysis. The analytes were separated by HPLC, and the HPLC elute was split (1/4, v/v) to a mass spectrometer for structural elucidation and an Agilent 1100 series 96-well fraction collector for determination of radioactivity of [^{14}C]venetoclax and metabolites. The radioactivity recovery in the processed plasma sample was ~84%.

Fecal homogenate were pooled across subjects at each time point prior to processing. The pooled fecal samples were extracted with 20 mL of acetonitrile/methanol (1/1, v/v), followed by centrifugation at 1875 *g* for 30 min at 4°C. The extraction was repeated twice, then once more with half the volume (10 mL), followed by centrifugation each time. Aliquots of extracted sample were subjected to LSC analysis for total radioactivity. All the supernatants were combined and concentrated under nitrogen flow at room temperature in glass tubes. The concentrated samples (~10 mL) were combined with 5 mL of DMSO. The resulting solution was vortexed, sonicated and centrifuged. An aliquot was subjected to HPLC-MS-radioflow analysis. Another aliquot of solution was subjected to LSC analysis for extraction recovery calculation. The overall radioactivity recovery for fecal samples ranged from 65.2-91.2%.

Urine samples were not analyzed due to negligible radioactivity (<0.1% of the administered dose) in the samples.

Method for Metabolite Profiling and Identification

Radiolabeled components in plasma or fecal samples were profiled following separation by HPLC and detection by fraction collection into 96-well LUMA plates (Perkin Elmer, Waltham, MA) and subsequent radiocounting analysis using Perkin Elmer TopCount NXT system. The HPLC system consisted of a Thermo Accela UHPLC system (Thermo Scientific, Waltham, MA) with Accela autosampler and 1250 Series binary pump. The HPLC system was interfaced with a mass spectrometer. The HPLC eluent was split in a ratio of 1 to 4; about 200 µL/min of flow was diverted to mass spectrometer source and ~800 µL/min flow was collected using Agilent 1100 fraction collection system set at 0.32 min interval per well collection. The chromatographic separation of metabolites in plasma and feces was achieved at room temperature on an Phenomenex Synergi Polar-RP, 5 µm, 4.6 x 250 mm HPLC column. Mobile phases were A: 25 mM ammonium formate aqueous solution, pH 3.5; and B: 100% acetonitrile. The flow rate was maintained at 1.0 mL/min. The gradient was as follows: 0-5 min: 30%-40% B; 5-60 min: 40%-50% B; 60-70 min: 50%-80% B; 70-80 min: 80% B; 80-82min: 80%-100% B; 82-85 min: 100% B; 85-87 min: 100-30% B; 87-90 min: 30% B. Mobile phase A was changed to 25 mM ammonium formate aqueous solution, pH 6.5 for blank human plasma sample spiked with M27 in order to confirm the pH dependent on-column formation of degradation product from M27. The high resolution MS and MS^n acquisitions were performed with a Thermo Scientific LTQ Orbitrap mass spectrometer, fitted with an ESI source. The mass spectrometer was set for a full scan and data- or list-dependent scan modes with mass resolution at 30,000 for the full scan and 7500 for MS^n scans. Typical source parameters were set as follows: sheath gas 45.0; auxiliary gas 0; ESI Source +4500 Volts; capillary temperature 350°C; capillary voltage 37 V; tube lens 135 V. The instrument was calibrated daily using external calibration solution containing caffeine, buspirone, and clarithromycin (1 µM in MeOH/H_2O). Typical mass errors of analytes

relative to theoretical masses are less than ± 5 parts per million (ppm) in daily operations. Thermo Xcalibur 3.0.63 was used for MS data processing.

Pharmacokinetic Calculations

Values for the pharmacokinetic parameters of total radioactivity, venetoclax, and M27 were determined using noncompartmental methods in SAS version 9.3 (SAS Institute Inc., Cary, NC). Parameters that were estimated included the maximum plasma concentration (C_{max}), the time to C_{max} (T_{max}), the apparent terminal phase elimination rate constant (β), the terminal phase elimination half-life ($t_{1/2}$), and the area under the concentration-time curve from time 0 to the last measureable time point (AUC_t), 48 hours (AUC_{0-48}), and to infinite time (AUC_∞).

Metabolism of Venetoclax by Human Fecal Homogenate.

Fresh fecal samples were collected from two healthy male volunteers. Aliquots of specimen (approx. 1 gram) were placed into pre-weighed 15 mL centrifuge tubes with screw caps. The sample tubes were kept in an AnaeroPouch (Mitsubishi Gas Chemical Company, Inc., Tokyo, Japan) with a PouchAnaero anaerobic gas generating system and an RT AnaeroIndicator before transferring to a CO_2 filled Aldrich AtmosBag (glove bag) that was connected to a CO_2 cylinder to create an anaerobic environment. An RT AnaeroIndicator was placed inside the bag to monitor the anaerobic conditions. Dulbecco's phosphate buffered saline (DPBS) was degassed by bubbling nitrogen gas through the solution overnight. The fecal samples were diluted with DPBS to a concentration of ~100 mg/mL under a CO_2 atmosphere. The samples were mixed by vortexing to break up solid matter. An aliquot of fecal homogenate (1.5 mL) was added to a 2 mL Corning cryogenic vials containing 10 μM of venetoclax. The vials were capped, vortexed and placed in an AnaeroPouch with a PouchAnaero anaerobic gas generating system and an RT AnaeroIndicator. The pouches were sealed before removing from the glove bag. The pouches

containing the sample vials were placed in a 37°C water bath for 48 hour. Anaerobic conditions were maintained throughout the study as shown by the RT AnaeroIndicator. At the end of the incubations, the samples were mixed with 1.5 mL of acetonitrile/methanol (3/1, v/v). After centrifugation at 1875 *g* for 30 min (4°C) , aliquots of supernatants were injected for HPLC-MS analysis.

Metabolism of Venetoclax and M5 by Recombinant CYP3A4.

Venetoclax and M5 was each incubated with recombinant CYP3A4 enzyme (Corning, NY) in the presence of nicotinamide adenine dinucleotide phosphate (NADPH). The incubation mixture (100 µL) included the substrate (20 µM for venetoclax and 100 µM for M5), recombinant CYP3A4 (100 pmol/mL) in 100 mM phosphate buffer at pH 7.4. After a 5 minute pre-warm in 37°C water bath, NADPH was added to initiate the reaction (NADPH final concentration 1 mM). Incubations were conducted in duplicate for 90 min for the incubations with venetoclax and 60 min for the incubations with M5. The reaction was stopped by the addition of 100 µL of acetonitrile to the incubation mixture with venetoclax or 400 µL of acetonitrile/methanol (1/1, v/v) to the incubation mixture with M5. The mixture was centrifuged at 1875 *g* for 30 min at 4°C. Aliquots of the supernatant were subjected to HPLC-MS analysis.

Quantitation of Venetoclax and M27 in Plasma

Specific and sensitive bioanalytical assays have been developed and validated for the quantitative determination of venetoclax in human plasma. The concentration of metabolite M27 was determined in human plasma sample using a non-validated method. Venetoclax and M27 were extracted from human plasma using the following liquid-liquid extraction technique: 100 µL of plasma was mixed with 50 µL of internal standard (d8-venetoclax) prior to the addition of 600 µL of 1/1 (v/v) hexane/ethyl acetate. After extraction, approximately 400 µL of the organic

layer was transferred to an injection plate for drying down under a stream of room temperature nitrogen gas. The concentrated extract was reconstituted with appropriate reconstitution solutions (1/1 (v/v) acetonitrile/water for venetoclax; DMSO for M27) prior to being injected onto HPLC-MS/MS. Detection was performed in the multiple reaction monitoring (MRM) mode at *m/z* 868 → 321 for venetoclax, *m/z* 876 → 329 for d8-venetoclax (the internal standard of venetoclax) and *m/z* 882 → 634 for M27. The chromatographic separation of the analytes from the co-extracted matrix components was achieved with a reverse-phase analytical column (Waters Atlantis dC18, 2.1x50 mm, 3 µm) running under isocratic condition (55/45 (v/v) acetonitrile/water with 0.1% formic acid). Analysis was performed on AB SCIEX mass spectrometers (4000 for venetoclax and 5500 for M27) (Applied Biosystems, Foster City, CA) with a Turbo Ion Spray interface operated under positive ion mode. The peak areas of all components of interest were determined using Sciex Analyst™ software. The concentration of each sample was calculated by least squares linear regression analysis of the peak area ratio (compound / internal standard) of the spiked human plasma standards versus concentration.

Results

Plasma Concentration-Time Profiles

Following a single oral 200 mg dose of [^{14}C]venetoclax in human, the mean plasma concentration-time profiles and pharmacokinetic parameters of total radioactivity, venetoclax and its major metabolite, M27, are shown in Figure 1 and Table 1 respectively. Venetoclax reached maximum plasma concentrations (T_{max}) at a median of 5 hours and had a mean C_{max} and $t_{1/2}$ (terminal phase elimination half-life) of 1.4 µg/mL and 23 hours, respectively. The total radioactivity-time profile was similar to that of venetoclax alone, but the AUC_{∞} was greater (35.4 µg-eq•h/mL versus 20.1 µg•h/mL), consistent with the presence of metabolites. The M27

metabolite reached peak concentrations at approximately 12 hours and had a terminal phase elimination half-life of ~59 hours.

Excretion of Radioactivity

The mean cumulative recovery of total radioactivity (as percentage of the administered dose) in urine and feces after a single oral dose of 200 mg venetoclax containing 100 μCi [^{14}C]venetoclax to four healthy subjects is represented in Figure 2. Mean (±S.D.) recovery of total radioactivity through 216 hours post dose was 100% (± 5%) with recovery in individual subjects ranging from 95 to 105%. The radioactivity was primarily eliminated in feces (100% ± 5%). Less than 0.1% of the administered dose was eliminated in urine.

Metabolite Profiles of [^{14}C]Venetoclax in Circulation and Excreta

Plasma. A representative HPLC radiochromatogram of [^{14}C]venetoclax and its metabolites in pooled human plasma (using the Hamilton method with t = 0-48 hour) is shown in Figure 3. Venetoclax was the primary component in plasma, representing 72.6% of total drug related material within 48 hours. The peak at 69.3 minutes in the radiochromatogram (labeled as **D** in Figure 3, *m/z* 898.2996) was also observed in blank human plasma spiked with M27 (Figure 4) under acidic HPLC conditions (pH3.5). This peak disappeared when the pH of mobile phase was changed from 3.5 to 6.5, suggesting that this component is not a product of in vivo metabolism but appears to be an on-column degradation product from M27 under acidic conditions (pH3.5). M27 was identified as a major human metabolite representing 12% of drug related material in plasma (sum of M27 and D). The degradation product (D) exhibited a protonated molecular ion at 898.2996 in electrospray positive ionization mode. The measured accurate mass suggested a molecular formula of $C_{45}H_{47}ClN_7O_8S^+$, with the addition of one oxygen atom to the M27 molecular formula. In the full scan mass spectrum, a pronounced in-source fragment at 880.2890

(loss of water) was also observed. The collision induced dissociation of *m/z* 880 generated three main fragments at m/z 650.2018, 565.1995, and 335.1133, which were assigned as indicated in supplemental Figure 4. The fragment ions at 650.2018, 565.1995 and 335.1133 were 14, 12, 14 mass units more than the corresponding fragment ions of the parent compound, respectively. Based on these MS^2 data, The degradation peak was proposed to be a product with a hydroxylation/dehydrogenation at 3 position of piperazine ring and hydroxylation at 6 position of cyclohexenyl ring. The formation mechanism of the degradation peak is proposed as shown in Supplemental Figure 5. M27 under mild acidic condition could undergo hydrolytic cleavage via nucleophilic addition of water and form carbinolamine intermediate leading to the formation of degradation product. In addition, two early eluting peaks were detected, each representing <10% of drug related material in plasma. These two early eluting peaks were retained in the column by utilizing different chromatographic conditions. Under both positive and negative ionization conditions, no ions were observed that could be related to the parent compound. Unambiguous identification could not be made.

Feces

The representative HPLC radiochromatogram of pooled human feces is shown in Figure 6. The administered [^{14}C]venetoclax was primarily recovered in feces as metabolites (78.6% of the administered dose), whereas 20.8% of the administered dose was recovered as the intact parent drug. The most significant metabolites in feces were M34 (oxidation, sulfation, and reduction of nitrophenyl), M30 (reduction of nitrophenyl), and M16 (oxidation and sulfation) representing 16.9%, 12.9% , and 8.7% of the administered dose, respectively. Other minor metabolites detected in feces included M2, M5, M14, M17, M18, M23, M27, M31, M32, M33, M35, M36, M37, Unknown 3 and Unknown 4, each representing <8.3% of the administered dose.

Metabolites M3, M4, M7, M10, M19, M22, M24, M25, M38, M39, M40, M41, M42, M43, M44 and M45 were only detected by LC-MS. The unambiguous identification of Unknown 3 peak could not be made, but it is thought that the metabolites comprising this region are polar metabolites and could be originated from the release of sulfonyltetrahydropyranylmethylnitro-aniline motif and further metabolism. The amount of venetoclax and metabolites in feces, expressed as the mean percentage of the administered dose, is tabulated in Table 2. The proposed metabolic scheme for venetoclax in humans is shown in Figure 7.

Structural Characterization of Venetoclax and Metabolites

Metabolites of venetoclax were characterized using a combination of positive ionization high resolution full scan MS and product ion scan (MS/MS) analyses (Supplemental Figure 1). The chemical structures of metabolites M3, M5, M6, M14, and M27 were confirmed by comparing the chromatographic retention time and mass spectral fragmentations with that of the reference standards. The chemical structures of M2 and M18 were confirmed by one dimensional NMR spectra (Supplemental Figure 2). Chemical structures of other metabolites were proposed based on high resolution MS/MS fragmentation pattern analysis. The measured accurate masses and characteristic fragment ions are listed in Table 3. The measured accurate masses and characteristic fragment ions and descriptions for metabolites that were only detected by LC/MS are listed in Supplemental Table 1.

Venetoclax. Venetoclax yielded a protonated molecular ion $[M+H]^+$ at *m/z* 868.3264 (chemical formula $C_{45}H_{51}ClN_7O_7S^+$) in positive ion mode. Collision-induced dissociation of venetoclax generated fragment ions at *m/z* 636.2235 (loss of chlorophenyldimethyl-cyclohexenyl moiety), 553.2363 (cleavage of amide bond with the loss of benzenesulfonamide moiety), 321.1346 (loss

of chlorophenyltrimethyl-cyclohexenyl and benzenesulfonamide moieties), and 295.1553 (further loss of CO and plus 2H from *m/z* 321.1346).

M2. M2 was detected in plasma and feces with a protonated molecular ion at *m/z* 884.3219. The predicted molecular formula was $C_{45}H_{51}ClN_7O_8S^+$. Collision-induced dissociation of M2 generated major fragment ions at *m/z* 636.2224 and 321.1349, which were same (within 5 ppm mass error) with the corresponding fragments from the parent drug. M2 was assigned as a hydroxylated metabolite of venetoclax with hydroxylation occurring at methyl group of dimethylcyclohexenyl moiety. The structure of M2 was further confirmed by one and two dimensional NMR spectra**.**

M5. M5 was detected in plasma and feces with a protonated molecular ion of *m/z* 884.3214. Measured accurate mass data suggested the molecular formula of $C_{45}H_{51}ClN_7O_8S^+$. Collision-induced dissociation of M5 generated the fragment ions at *m/z* 866.3095 (loss of water), 636.2225 and 634.2072. The fragment ions at *m/z* 636.2225 and 634.2072 was same with or 2 mass units less than the corresponding fragments of the parent compound. M5 was assigned as a hydroxylated metabolite of venetoclax with hydroxylation occurring at 6 position of cyclohexenyl ring. The structure of M5 was further confirmed by comparing MS/MS fragmentation pattern and chromatographic retention time with the reference standard.

M6. M6 was detected in plasma with a protonated molecular ion of *m/z* 884.3220. Measured accurate mass data suggested the molecular formula of $C_{45}H_{51}ClN_7O_8S^+$. Collision-induced dissociation of M6 generated the fragment ion *m/z* 652.2177; this fragment was 16 mass units more than the corresponding fragment of the parent drug, suggesting that oxidation occurred at pyrrolopyridinyloxypiperazinylbenzamide moiety. M6 was assigned as the piperazine-*N*-oxide of

venetoclax. The structure of M6 was further confirmed by comparing MS/MS fragmentation pattern and chromatographic retention time with the reference standard.

M14. M14 was detected in feces with a protonated molecular ion at *m/z* 882.3057. Measured accurate mass data suggested the molecular formula of $C_{45}H_{49}ClN_7O_8S^+$. Collision-induced dissociation of M14 generated the fragment ions at *m/z* 650.2025 and *m/z* 335.1135; these fragments were 14 mass units more than the corresponding fragments of the parent drug, suggesting the modification at the pyrrolopyridinyloxypiperazinylbenzamide moiety. M14 was assigned as a 2-ketopiperazine metabolite of parent drug. The structure of M14 was further confirmed by comparing MS/MS fragmentation pattern and chromatographic retention time with the reference standard.

M16. M16 was detected in feces with a protonated molecular ion at *m/z* 964.2777. Measured accurate mass data suggested the molecular formula of $C_{45}H_{51}ClN_7O_{11}S_2^+$. Collision-induced dissociation of M16 generated the fragment ions at *m/z* 884.3198 (loss of SO_3), 636.2230, 569.2311 and 321.1345. The fragment ions at 636.2230 and 321.1345 were consistent with the corresponding fragments of the parent drug and the fragment ion at 569.2311 was 16 mass units more than the corresponding fragment of the parent drug. These fragments suggested that oxidation occurred at the chlorophenyldimethylcyclohexenyl moiety. M16 was proposed to be a hydroxylation and sulfation metabolite of parent drug.

M17. M17 was detected in plasma and feces with a protonated molecular ion at *m/z* 900.3185. Measured accurate mass data suggested the molecular formula of $C_{45}H_{51}ClN_7O_9S^+$. Collision-induced dissociation of M17 generated fragment ions at *m/z* 668.2135 and 321.1346. The fragment ion at 668.2135 was 32 mass units more than the corresponding fragment of the parent drug and the fragment ion at 321.1346 was consistent with the corresponding fragment of the

DMD Fast Forward. Published on December 19, 2016 as DOI: 10.1124/dmd.116.071613
This article has not been copyedited and formatted. The final version may differ from this version.

parent drug, suggesting that modification occurred at the tetrahydropyranylmethyl-aminonitrophenylsulfonylamide moiety. M17 was proposed to be formed from oxidation at the α-methylene position of the tetrahydropyranyl ring, followed by hydrolytic ring opening.

M18. M18 was detected in feces and plasma with a protonated molecular ion at *m/z* 898.3020. Measured accurate mass suggested the molecular formula of $C_{45}H_{49}ClN_7O_9S^+$. Collision-induced dissociation showed fragment ions at *m/z* 636.2232 and 321.1346; these fragments remained the same (within 5 ppm) with the corresponding fragments of the parent drug, suggesting that modification occurred at the chlorophenyldimethylcyclohexenyl moiety. M18 structure was assigned as the cyclohexenyl carboxylic acid of parent drug. The structure of M18 was further confirmed by one and two dimensional NMR spectra**.**.

M23. M23 was detected in feces with a protonated molecular ion at *m/z* 916.3124. Measured accurate mass suggested the molecular formula of $C_{45}H_{51}ClN_7O_{10}S^+$. Collision-induced dissociation of M23 showed fragment ion at *m/z* 898.2997, resulting from loss of H_2O. M23 was proposed to be the tri-hydroxylated metabolite of parent drug.

M27. M27 was detected in plasma and feces with a protonated molecular ion at *m/z* 882.3042. Measured accurate mass suggested a molecular formula of $C_{45}H_{49}ClN_7O_8S^+$. Collision-induced dissociation of M27 showed fragment ions at *m/z* 864.2936 (loss of water), 634.2056, and 567.2184. The fragment ions at 634.2056 and 567.2184 were 14 mass units more than the corresponding fragments of the parent drug, suggesting that modification occurred at pyrrolopyridinyloxy-piperazinylbenzamide and chlorophenyldimethylcyclohexenyl moiety. M27 was assigned as the metabolite with oxidation at 6 position of cyclohexenyl ring followed by cyclization at the α-carbon of piperazine. The structure of M27 was further confirmed by comparing MS/MS fragmentation pattern and chromatographic retention time with the reference

standard. With chiral separation, absolute stereochemistry of M27 was determined to be one of syn-configuration (10aR, 11aS) (Supplemental Figure 3).

M30. M30 was detected in feces with a protonated molecular ion at *m/z* 838.3519. Measured accurate mass suggested a molecular formula of $C_{45}H_{53}ClN_7O_5S^+$. Collision-induced dissociation of M30 showed the key fragment ions at *m/z* 606.2493, *m/z* 321.1347, and *m/z* 295.1555. The fragment ion at 606.2493 was 30 mass units less than the corresponding fragment of the parent drug, suggesting the reduction of the nitrophenyl moiety to an aniline. M30 was tentatively assigned as a nitro reduction metabolite of parent drug.

M31. M31 was detected in feces with a protonated molecular ion at *m/z* 854.3466. Measured accurate mass suggested a molecular formula of $C_{45}H_{53}ClN_7O_6S^+$. Collision-induced dissociation of M31 showed the key fragment ions at *m/z* 606.2488, *m/z* 569.2312, *m/z* 321.1345, and *m/z* 295.1550 suggesting that mono-oxidation occurred at chlorophenyldimethylcyclohexenyl moiety, followed by reduction of nitrophenyl moiety. M31 was proposed to be an oxidation and nitro reduction metabolite of parent drug.

M32. A metabolite peak with a protonated molecular ion at *m/z* 854.3464 was observed in feces. Measure accurate mass suggested the molecular formula of $C_{45}H_{53}ClN_7O_6S^+$. Collision-induced dissociation of M32 showed the key fragment ions at *m/z* 836.3355 (loss of water) and *m/z* 606.2484. These data suggested that the mono-oxidation occurred at chlorophenyldimethylcyclohexenyl moiety, followed by the reduction of the nitrophenyl moiety. M32 was proposed to be an hydroxylation and nitro reduction metabolite of parent drug.

M33. A metabolite peak with a protonated molecular ion at *m/z* 854.3464 was observed in feces. Measured accurate mass suggested a molecular formula of $C_{45}H_{53}ClN_7O_6S^+$. Collision-induced dissociation of M32 showed the key fragment ions at *m/z* 836.3354 (loss of water) and *m/z*

606.2489. These data suggested that oxidation occurred at chlorophenyldimethylcyclohexenyl moiety, followed by reduction of nitrophenyl moiety. M33 was proposed to be an hydroxylation and nitro reduction metabolite of parent drug.

M34. A metabolite peak with a protonated molecular ion at *m/z* 934.3040 was observed in feces. Measured accurate mass suggested a molecular formula of $C_{45}H_{53}ClN_7O_9S_2^+$. Collision-induced dissociaiton of M34 showed the key fragment ions at *m/z* 854.3462 (loss of SO3), *m/z* 606.2491, *m/z* 569.2313 and *m/z* 321.1347. These data suggest that the oxidation occurred at chlorophenyldimethylcyclohexenyl moiety, followed by sulfation and reduction of nitrophenyl moiety. M34 was proposed to be an hydroxylation, sulfation, and nitro reduction metabolite of parent drug.

M35. A metabolite peak with a protonated molecular ion at *m/z* 854.3464 was observed in feces. Measured accurate mass suggested a molecular formula of $C_{45}H_{53}ClN_7O_6S^+$. Collision-induced dissociation of M35 showed the fragment ions at *m/z* 837.3220 (loss of water), *m/z* 606.2492, *m/z* 569.2314, *m/z* 321.1347, and *m/z* 295.1550, suggesting that oxidation occurred at chlorophenyldimethylcyclohexenyl moiety, followed reduction of nitrophenyl moiety. M35 was tentatively assigned as a hydroxylation and nitro reduction metabolite of parent drug.

M36. A metabolite peak with a protonated molecular ion at *m/z* 870.3415 was observed in feces. Measured accurate mass suggested a molecular formula of $C_{45}H_{53}ClN_7O_7S^+$. Collision-induced dissociation of M36 showed the key fragment ions at *m/z* 852.3302 (loss of water) and *m/z* 606.2489, suggesting that di-oxidation occurred at chlorophenyldimethylcyclohexenyl moiety, followed by reduction of nitrophenyl moiety. M36 was tentatively assigned as a di-hydroxylation and nitro reduction metabolite of parent drug.

M37. M37 was detected in feces with a protonated molecular ion at *m/z* 870.3416, suggesting a molecular formula of $C_{45}H_{53}ClN_7O_7S^+$. Collision-induced dissociation of M37 showed the key fragment ions at *m/z* 852.3302 (loss of water), 834.3199 (loss of second water) and *m/z* 606.2489, suggesting that di-oxidation occurred at chlorophenyldimethylcyclohexenyl moiety, followed by reduction of nitrophenyl moiety. M37 was tentatively assigned as a di-hydroxylation and nitro reduction metabolite of parent drug.

Quantification of M27 Following Multiple Oral Dosing in Human and Non-clinical Safety Species

As M27 was determined to be a major human metabolite, plasma concentration of M27 was measured at steady state in human and non-clinical species in order to assess metabolite coverage. In human, steady state plasma samples from CLL or NHL patients receiving multiple doses of 400 mg/day were selected for analysis. In two non-clinical species used in the toxicity assessment of venetoclax, steady state plasma samples (5 days) at maximal tolerated dose (MTD, 600 mg/kg in mice and 100 mg/kg in dogs) were selected for analysis. The measured concentrations (C_{max}) and AUCs of M27 are listed in Supplemental Table 2. M27 exposure was 14.1 µg•hr/mL in human. M27 was also detected in mice and dogs but at lower exposure than in human. M27 exposures were 0.760 and 1.27 µg•hr/mL in mice and dogs, respectively. The exposure multiples for M27 were calculated as 0.05x and 0.09x in mice and dogs, respectively. Therefore, M27 is determined to be a disproportionate human metabolite per ICH M3 R2 and FDA Guidance on Safety Testing of Drug Metabolites.

Metabolism of Venetoclax by Human Fecal Homogenate

A nitro reduction metabolite M30 that was observed in human feces after a single oral dose of venetoclax was not detected in incubations of venetoclax in hepatic in vitro systems (liver

microsomes, hepatocytes) under aerobic conditions. This experiment was conducted to evaluate if M30 was formed by human gut bacteria. Venetoclax was incubated in freshly prepared human fecal homogenate under anaerobic conditions. Extracted ion chromatograms of M30 and venetoclax (Figure 8) showed that venetoclax underwent reduction of the nitrophenyl group to form M30 after a 48 hour incubation at 37°C. This result suggested that nitro reduction metabolites observed in human feces after a single oral dose of venetoclax were likely formed by human gut bacteria.

Metabolism of Venetoclax and M5 by Recombinant CYP3A4

In vitro enzyme phenotyping (CYPs and FMOs) study with venetoclax suggested that CYP3A4 is the primary enzyme to metabolize venetoclax. Therefore CYP3A4 was used to investigate the formation pathway of M27. Following in vitro incubations of venetoclax in recombinant CYP3A4 enzyme, several oxidative metabolites including M2, M3, M4, M5, M6, M14, and M18 were identified. This was consistent with the metabolites observed from incubations of venetoclax in human liver microsomes (HLM). M27 was not detected from this incubation or incubations in HLM, which is likely due to the low turnover of venetoclax in hepatic in vitro systems. However, M27 was detected in in incubations of M5 with recombinant CYP3A4. Based on these experimental data, M27 was proposed to be formed via mono-oxidation of venetoclax on the 6-position of the cyclohexenyl moiety to give M5, followed by enzyme-mediated cyclization at the α-carbon of piperazine (Figure 5).

Discussion

Following an oral administration of [^{14}C]venetoclax in healthy subjects, mean total recovery was 100% (± 5%) over 216 hours post dose. Feces was the major route of excretion, accounting for ~100% of the administered dose, while urinary excretion was minimal (<0.1% of the

administered dose). The rate of excretion was rapid, with majority (~81%) of the administered dose recovered within 96 hours. Excretion of the majority of the dose via feces is consistent with that observed in preclinical species (mouse, rat and dog) in which the fraction of the dose recovered in feces was also high (79.1-93.6%, Manuscript in preparation).

Venetoclax is well absorbed (>65% based on amounts of total metabolites minus M30 in feces) with a median T_{max} of 5 hours after oral administration. The plasma concentration-time profile for total radioactivity was similar to that of venetoclax alone (measured by LC-MS/MS), but the AUC_{∞} was greater, indicating the presence of metabolites in circulation. Metabolite profiling showed that unchanged parent drug was the major component, accounting for 72.6% of the total drug related material in pooled plasma ($AUC_{0\text{-}48\ hours}$). Two early eluting radiochromatographic peaks (unknowns, as yet uncharacterized peaks), M27 (4-[(10aR,11aS)-7-(4-chlorophenyl)-9,9-dimethyl-1,3,4,6,8,10,10a,11a-octahydropyrazino[2,1-b][1,3]benzoxazin-2-yl]-N-[3-nitro-4-(tetrahydropyran-4-ylmethylamino)phenyl]sulfonyl-2-(1H-pyrrolo[2,3-b]pyridin-5-yloxy)benzamide), and a peak eluted at 69.3 minutes were observed in pooled plasma. As described in the Result section, the peak eluted at 69.3 minutes was determined to be an on-column degradation product from M27 under acidic conditions (pH 3.5). M27 represented 12.0% of total drug related material in plasma (combined area of M27 and its degradation product). Two early eluting unknown peaks each represented less than 10% of total drug related material in plasma. Evaluation of AUC_{∞} data showed that the sum of venetoclax and M27 AUC values (measured by LC-MS/MS method) was approximately 100% of the ^{14}C AUC_{∞} (measured by LSC) in plasma, indicating that the parent compound and M27 accounted for a majority of the total drug-related material, and two early eluting unknown peaks were minor metabolites with insignificant contribution to overall AUC of radioactivity, and therefore, unlikely to contribute to

pharmacological activity and cause safety concerns. M27 exhibited a protonated molecular ion at 882.3042 in electrospray positive ionization mode. Collision-induced dissociation of *m/z* 882 generated three main fragments at *m/z* 864.2936, 634.2056, and 567.2184, which were assigned as indicated in Supplemental Figure 1. Several possible structures can be proposed based on the LC-MS/MS data that include 1) the hydroxylation in the piperazine ring and desaturation of cyclohexenyl moiety; 2) the desaturation of carbon-carbon bond of the piperazine ring and hydroxylation in the cyclohexenyl moiety; 3)desaturation of C-N bonds of the piperazine ring followed by cyclization via hydroxylation group on the 6-position of cyclohexenyl moiety. Several synthetic standards were made in order to confirm the chemical structure of M27. By comparing MS/MS fragmentation patterns and chromatographic retention time with the synthetic standards, it was confirmed M27 was formed through oxidation at 6 position of cyclohexenyl ring (M5) followed by cyclization at the α-carbon of piperazine, which is consistent with the third proposal. Enzymatically mediated fused ring formations are relatively uncommon, but have been observed for other drugs (Liu et al., 2007) (Takahashi et al., 2015). The cyclization is proposed to be driven by enzymatic nucleophilic (hydroxyl group) attack to electrophilic atoms (iminium carbon) (Erve, 2008). In addition, chiral LC/MS analysis with synthetic standard also confirmed that M27 is one of the two syn-configuration stereoisomers. As demonstrated in the PK profile, peak plasma concentrations of M27 were achieved at a later time point (12 hour post dose) as compared to parent drug (5 hour post dose), and M27 exhibited a longer elimination half-life (58.8 hr, approximately 2.5 fold longer than venetoclax), and is considered to be elimination rate-limited with a low intrinsic clearance. M27 was primarily eliminated by hepatobiliary route (1.3% of dose recovered in feces) in human. Relatively high plasma levels of M27 could be explained by the low intrinsic clearance of M27 consistent with long elimination

half-life ($t_{1/2}$=~59 hours). M27 has been observed in steady state plasma samples in mice and dogs dosed at MTDs of venetoclax for 5 days but the exposure in human plasma at 400 mg/day was not covered by those measured in mice and dogs, with metabolite coverage of 0.05x, and 0.09x, respectively. Based on these observations, M27 is a disproportionate metabolite in human per ICH M3 (R2) and FDA Guidance on Safety Testing of Drug Metabolites. M27 is not expected to be pharmacologically active in vivo as the in vitro potency is at least 58-fold less than venetoclax (AbbVie internal data). M27 was evaluated in a CEREP receptors binding panel including more than 75 receptors, ion channels, transporters, and is not expected to have clinically relevant off-target pharmacologic activity. In addition, M27 was negative in GLP in vitro Ames and chromosome aberration assays. Based on the foregoing nonclinical safety data indicating no additional safety risk for M27, as well as clinical safety data indicating that all findings are consistent with the expected mechanism of action of venetoclax, further safety evaluation for M27 was not conducted for the venetoclax indication of relapsed/refractory chronic lymphocytic leukemia (CLL).

Venetoclax was primarily cleared by hepatic metabolism (~66% of the administered dose). Biotransformation of venetoclax in human primarily involves enzymatic oxidation on the chlorophenyldimethyl cyclohexenyl moiety to form M2 (2-((1H-pyrrolo[2,3-b]pyridin-5-yl)oxy)-4-(4-((4'-chloro-5-(hydroxymethyl)-5-methyl-3,4,5,6-tetrahydro-[1,1'-biphenyl]-2-yl)methyl)piperazin-1-yl)-N-((3-nitro-4-(((tetrahydro-2H-pyran-4-yl)methyl)amino)phenyl)sulfonyl)benzamide), M3 (4-[4-[[2-(4-chlorophenyl)-3-hydroxy-4,4-dimethyl-cyclohexen-1-yl]methyl]piperazin-1-yl]-N-[3-nitro-4-(tetrahydropyran-4-ylmethylamino)phenyl]sulfonyl-2-(1H-pyrrolo[2,3-b]pyridin-5-yloxy)benzamide), M4 (hydroxylation on chlorophenyldimethyl-cyclohexenyl moiety) and M5 (4-[4-[[2-(4-

chlorophenyl)-6-hydroxy-4,4-dimethyl-cyclohexen-1-yl]methyl]piperazin-1-yl]-N-[3-nitro-4-(tetrahydropyran-4-ylmethylamino)phenyl]sulfonyl-2-(1H-pyrrolo[2,3-b]pyridin-5-yloxy)benzamide). These hydroxylated metabolites undergo either further oxidation to generate M18, M22, M25, and M27, etc. or sulfation to form M16. Venetoclax, its oxidative metabolites, and M16 also undergo nitro reduction to form reduction metabolites (M30, M34, etc.). M30 (2-((1H-pyrrolo[2,3-b]pyridin-5-yl)oxy)-N-((3-amino-4-(((tetrahydro-2H-pyran-4-yl)methyl)amino)phenyl)sulfonyl)-4-(4-((4'-chloro-5,5-dimethyl-3,4,5,6-tetrahydro-[1,1'-biphenyl]-2-yl)methyl)piperazin-1-yl)benzamide), the reductive metabolite of venetoclax (~13% of dose recovered in feces), showed similar physicochemical properties (lipophilicity, tPSA, etc.) as venetoclax, but is not detected in plasma suggesting these nitrophenyl reduction metabolites were likely not formed by the liver. Furthermore, M30 was formed from venetoclax upon incubations in freshly prepared human fecal homogenate under anaerobic conditions. This suggested gut bacteria may be responsible for nitro reduction of venetoclax. It is postulated that other nitro reduction metabolites including M34 were also formed by gut bacteria from M16 or venetoclax oxidative metabolites that were formed in the liver and excreted via bile into the feces. Gut bacteria are responsible for the biotransformation of many endogenous and exogenous molecules, usually involving reduction, hydrolysis, dehydroxylation, decarboxylation, etc. (Sousa et al., 2008; Klaassen and Cui, 2015; Shen et al., 2016). Several marketed drugs including nitrazepam, clonazepam, and misonidazole have been reported to undergo gut bacteria mediated nitro reduction resulting in the formation of primary amine metabolites (Koch et al., 1980; Elmer and Remmel, 1984; Takeno et al., 1990). Clostridium and eubacterium have been identified from human intestinal microbial flora as the anaerobic bacteria capable of producing nitroreductases and reducing nitro aromatic compounds (Rafil et al., 1991). Gut bacteria

mediated metabolism could lead to the formation of active or toxic metabolites, and therefore affect pharmacokinetics and therapeutic outcome of the parent drug. Nitrazepam, mentioned above, has been reported to induce teratogenicity via gut bacteria mediated reduction to 7-aminonitrazepam, followed by hepatic acetylation forming 7-acetylaminonitrazepam (Takeno and Sakai, 1991). The nitro reduction metabolites of venetoclax including M30, M34 were not expected to cause systemic or local effect because 1) these nitro reduction metabolites were not detected in human plasma, suggesting they are not absorbed to the systemic circulation following the formation in the intestine; 2) the clinical safety findings of venetoclax are consistent with the mechanism of action of venetoclax. 3) the structure-activity relationship analysis suggests that nitro reduction metabolites are significantly less pharmacological active as compared to venetoclax. The total amount of unchanged parent drug and its reduction metabolite M30 excreted in feces could be due to unabsorbed parent drug or biliary elimination of parent drug. In a bile duct cannulated rat ADME study after a single 5 mg/kg oral dose of venetoclax (Manuscript in preparation), about 14% and 65% of administered dose were recovered in bile and feces, and about 0.9% of the dose in bile was recovered as unchanged parent drug, which indicated that the unchanged venetoclax and M30 in human feces were likely due to unabsorbed parent drug. In addition, consistent with the minimal urinary excretion of parent drug in urine, mild and moderate renal impairment were found not to impact venetoclax exposures in a population pharmacokinetic analysis of 8 clinical studies (Jones et al., 2016).

In summary, this AME study with [^{14}C]venetoclax in healthy female subjects showed a rapid and good absorption of venetoclax (>65% of the administered dose), extensive metabolism, and complete excretion (100% of the administered dose) through fecal route. Venetoclax was predominantly cleared by metabolism, primarily through oxidation and further sulfation. Nitro

reduction metabolites observed in feces were likely formed by gut bacteria. The major disproportionate human metabolite M27 was not expected to have clinically relevant on- or off-target pharmacological activity.

Acknowledgements: Special thanks to Dr. Yu-Ming Pu for preparation of M3; Dr. Wenke Li, Dr. David R. Hill, and Dr. Benoit Cardinal-David for preparation of M5; Mr. Aaron Kunzer for preparation of M14; Dr. David R. Hill, Dr. Wenke Li and Dr. Steven R. Martinez for preparation of M27; Dr. David N. Whittern for the interpretation of NMR spectra; and Ms Ai-Duen Su for performing the incubations of M5 with recombinant CYP3A4 enzyme.

Authorship Contributions

Participated in research design: Liu, Lao, Wan, Salem, Wong

Conducted experiments: Michmerhuizen, Sawicki, Serby

Contributed new reagents: Vaidyanathan

Performed data analysis: Liu, Lao, Wan, Lee, Salem, Wong, Agarwal, Dunbar

Wrote or contributed to the writing of the manuscript: Liu, Salem, Michmerhuizen, Wan, Lee, de Morais, Sydor,

DMD Fast Forward. Published on December 19, 2016 as DOI: 10.1124/dmd.116.071613
This article has not been copyedited and formatted. The final version may differ from this version.

References

Agarwal SK, Hu B, Chien D, Wong SL, and Salem AH (2016a) Evaluation of Rifampin's Transporter Inhibitory and CYP3A Inductive Effects on the Pharmacokinetics of Venetoclax, a Bcl-2 Inhibitor: Results of a Single- and Multiple-dose Study. *Journal of clinical pharmacology* **56:**1335-1343.

Agarwal SK, Salem AH, Danilov AV, Hu B, Puvvada P, Gutierrez M, Chien D, and SoL. LW (2016b) Effect of Ketoconazole, a Strong CYP3A Inhibitor, on the Pharmacokinetics of Venetoclax, a Bcl-2 Inhibitor, in Patients with Non-Hodgkin Lymphoma. *British J Clin Pharmacol* DOI: 10.1111/bcp.13175.

Brown JE and Dunmore SJ (2007) Leptin decreases apoptosis and alters BCL-2 : Bax ratio in clonal rodent pancreatic beta-cells. *Diabetes/metabolism research and reviews* **23:**497-502.

Davids MS, Roberts A, Seymour JF, Pagel JM, Kahl BS, Wierda WG, Puvvada S, Kipps TJ, Anderson MA, Salem AH, Dunbar M, Zhu M, Peale F, Ross JA, Gressick L, Desai MB, Kim SY, Verfugo M, Humerickhouse RA, Gordon GB, and Gerecitano JF (2016) A phase 1 first-in-human study of venetoclax in patients with relapsed or refractory non-Hodgkin lymphoma. *J Clin Oncol* In press.

DiNardo C, Pollyea DA, Pratz K, Thirman MJ, Letai A, Frattini M, Jonas B, Leverson JD, Zhu M, Dunbar M, Falotico N, Kirby R, Agarwal S, Mabry M, Potluri J, Humerickhouse RA, Kantarjian HP, and Konopleva M (2015) A phase 1b study of venetoclax (ABT 199/GDC-0199) in combination with decitabine or azacitidine in treatment-naive patients with acute myelogenous leukemia who are ≥ 65 years and not eligible for standard induction therapy. *Blood* **15:**327.

Elmer GW and Remmel RP (1984) Role of the intestinal microflora in clonazepam metabolism in the rat. *Xenobiotica; the fate of foreign compounds in biological systems* **14:**829-840.

Erve JC (2008) Cyclic metabolites: chemical and biological considerations. *Current drug metabolism* **9:**175-188.

Hamilton RA, Garnett WR, and Kline BJ (1981) Determination of mean valproic acid serum level by assay of a single pooled sample. *Clinical pharmacology and therapeutics* **29:**408-413.

Jaglowski S and Jones JA (2011) Choosing first-line therapy for chronic lymphocytic leukemia. *Expert review of anticancer therapy* **11:**1379-1390.

Jones AK, Freise KJ, Agarwal S, Humerickhouse RA, Wong SL, and Salem AH (2016) Clinical Predictors of Venetoclax Pharmacokinetics, a Selective BCL-2 inhibitor, in Chronic Lymphocytic Leukemia and Non-Hodgkin's Lymphoma Patients: A Pooled Population Pharmacokinetic Analysis. *AAPS jounal* **18:**192-202.

Klaassen CD and Cui JY (2015) Review: Mechanisms of How the Intestinal Microbiota Alters the Effects of Drugs and Bile Acids. *Drug metabolism and disposition: the biological fate of chemicals* **43:**1505-1521.

Koch RL, Beaulieu BB, Jr., and Goldman P (1980) Role of the intestinal flora in the metabolism of misonidazole. *Biochemical pharmacology* **29:**3281-3284.

Konopleva M, Pollyea DA, Potluri J, Chyla B, Hogdal L, Busman T, McKeegan E, Salem AH, Zhu M, and Ricker JL (2016) Efficacy and Biological Correlates of Response in a Phase II Study of Venetoclax Monotherapy in Patients with Acute Myelogenous Leukemia. *Cancer Discovery* **6**: 1106-1117

Liu DQ, Arison BH, Stearns RA, Kim D, and Vincent SH (2007) Characterization of two cyclic metabolites of sitagliptin. *Drug metabolism and disposition: the biological fate of chemicals* **35:**521-524.

Moreau P, Chanan-Khan A, Roberts AW, Agarwal S, Facon T, Kumar S, Touzeau C, Darden D, Morris L, Ross J, Salem AH, Munasinghe W, Zhu M, Leverson JD, Maciag P, Enschede SH, Verdugo M, Humerickhouse RA, and Harrison S (2015) Safety and efficacy of

venetoclax (ABT-199/GDC-0199) in combination with bortezomib and dexamethasone in relapsed/refractory multiple myeloma: phase 1b results. *Blood* **126:** 3038.

Rafil F, Franklin W, Heflich RH, and Cerniglia CE (1991) Reduction of nitroaromatic compounds by anaerobic bacteria isolated from the human gastrointestinal tract. *Applied and environmental microbiology* **57:**962-968.

Roberts AW, Davids MS, Pagel JM, Kahl BS, Puvvada SD, Gerecitano JF, Kipps TJ, Anderson MA, Brown JR, Gressick L, Wong S, Dunbar M, Zhu M, Desai MB, Cerri E, Heitner Enschede S, Humerickhouse RA, Wierda WG, and Seymour JF (2016) Targeting BCL2 with Venetoclax in Relapsed Chronic Lymphocytic Leukemia. *The New England journal of medicine* **374:**311-322.

Robertson LE, Plunkett W, McConnell K, Keating MJ, and McDonnell TJ (1996) Bcl-2 expression in chronic lymphocytic leukemia and its correlation with the induction of apoptosis and clinical outcome. *Leukemia* **10:**456-459.

Salem AH, Agarwal S, Dunbar M, Nuthalapati S, Chien D, Freise KJ, and Wong SL (2016a) Effect of Low and High Fat Meals on the Pharmacokinetics of Venetoclax, a Selective First-in-Class Bcl-2 Inhibitor. *Journal of clinical pharmacology* **56:**1355-1361.

Salem AH, Agarwal SK, Dunbar M, Enschede SLH, Humerickhouse RA, and Wong SL (2016b) Pharmacokinetics of Venetoclax, a Novel BCL‐2 Inhibitor, in Patients with Relapsed or Refractory Chronic Lymphocytic Leukemia or Non‐Hodgkin's Lymphoma. *The Journal of Clinical Pharmacology*. doi: 10.1002/jcph.821.

Shen J, Serby M, Reed A, Lee AJ, Zhang X, Marsh KC, Khatri A, Menon R, Kavestskaia O, and Fischer V (2016) Metabolism and Disposition of the Hepatitis C Protease Inhibitor Paritaprevir in Humans. *Drug metabolism and disposition: the biological fate of chemicals* **44:**1164-1173.

Shenoy PJ, Malik N, Sinha R, Nooka A, Nastoupil LJ, Smith M, and Flowers CR (2011) Racial differences in the presentation and outcomes of chronic lymphocytic leukemia and variants in the United States. *Clinical lymphoma, myeloma & leukemia* **11:**498-506.

Souers AJ, Leverson JD, Boghaert ER, Ackler SL, Catron ND, Chen J, Dayton BD, Ding H, Enschede SH, Fairbrother WJ, Huang DC, Hymowitz SG, Jin S, Khaw SL, Kovar PJ, Lam LT, Lee J, Maecker HL, Marsh KC, Mason KD, Mitten MJ, Nimmer PM, Oleksijew A, Park CH, Park CM, Phillips DC, Roberts AW, Sampath D, Seymour JF, Smith ML, Sullivan GM, Tahir SK, Tse C, Wendt MD, Xiao Y, Xue JC, Zhang H, Humerickhouse RA, Rosenberg SH, and Elmore SW (2013) ABT-199, a potent and selective BCL-2 inhibitor, achieves antitumor activity while sparing platelets. *Nature medicine* **19:**202-208.

Sousa T, Paterson R, Moore V, Carlsson A, Abrahamsson B, and Basit AW (2008) The gastrointestinal microbiota as a site for the biotransformation of drugs. *International journal of pharmaceutics* **363:**1-25.

Takahashi RH, Ma S, Robinson SJ, Yue Q, Choo EF, and Khojasteh SC (2015) Elucidating the Mechanisms of Formation for Two Unusual Cytochrome P450-Mediated Fused Ring Metabolites of GDC-0623, a MAPK/ERK Kinase Inhibitor. *Drug metabolism and disposition: the biological fate of chemicals* **43:**1929-1933.

Takeno S, Nakagawa M, and Sakai T (1990) Teratogenic effects of nitrazepam in rats. *Research communications in chemical pathology and pharmacology* **69:**59-70.

Takeno S and Sakai T (1991) Involvement of the intestinal microflora in nitrazepam-induced teratogenicity in rats and its relationship to nitroreduction. *Teratology* **44:**209-214.

Zenz T, Mertens D, Kuppers R, Dohner H, and Stilgenbauer S (2010) From pathogenesis to treatment of chronic lymphocytic leukaemia. *Nature reviews Cancer* **10:**37-50.

DMD Fast Forward. Published on December 19, 2016 as DOI: 10.1124/dmd.116.071613
This article has not been copyedited and formatted. The final version may differ from this version.

Disclosure Statement: All authors are employees/retirees of AbbVie and may hold AbbVie stock or stock options. Yanbin Lao is currently an employee at Eli Lilly and Company. AbbVie and Genentech/Roche provided financial support for the studies and participated in the design, study conduct, analysis and interpretation of data as well as the writing, review and approval of the publication. Venetoclax is being developed in a collaboration between AbbVie and Genentech/Roche.

DMD Fast Forward. Published on December 19, 2016 as DOI: 10.1124/dmd.116.071613
This article has not been copyedited and formatted. The final version may differ from this version.

Figures

DMD Fast Forward. Published on December 19, 2016 as DOI: 10.1124/dmd.116.071613
This article has not been copyedited and formatted. The final version may differ from this version.

Tables

Table 1. Mean (%CV) Pharmacokinetic Parameters of Venetoclax, M27 Metabolite and Total Radioactivity in Plasma After a Single Oral Dose of [^{14}C]Venetoclax

Parameter	Venetoclax (N = 4)	M27 (N = 4)	Total Radioactivity (N = 4)
T_{max} [a] (h)	5 (4 – 8)	12 (12 – 12)	5 (4 -10)
C_{max} (µg/mL)	1.41 (30)	0.28 (27)	1.57 (26.8)
$t_{1/2}$ [b] (h)	23.3 (4.4)	58.8 (32)	20.1 (68.7)
AUC_t (µg•h/mL)	20.0 (35)	14.9 (32)	--
AUC_∞ (µg•h/mL)	20.1 (35)	15.8 (32)	35.4 (39.2)
% AUC_{ext}	--	--	10.5 (19.4)
$AUC_{0\text{-}48h}$ (µg-eq•h/mL)	--	--	31.6 (38.4)

[a] T_{max} is presented as median (min – max).

[b] Harmonic mean (%CV).

Note: for total radioactivity, the units are µg-eq/mL for C_{max} and µg-eq•h/mL for AUC.

DMD Fast Forward. Published on December 19, 2016 as DOI: 10.1124/dmd.116.071613
This article has not been copyedited and formatted. The final version may differ from this version.

Table 2. Percentages of Venetoclax and Metabolites[a] in Human Feces Following a Single Oral Dose of 200 mg (100 μCi) of [^{14}C]Venetoclax (n=4)

Matrix	**Feces**							**Total**
Hours	**0-24**	**24-48**	**48-72**	**72-96**	**96-120**	**120-144**	**144-168**	**0-168**
Parent	1.06	4.57	10.13	2.26	0.83	1.29	0.69	20.8
M2/M17 /M33*	MS/MS/ ND	MS/MS/ 0.8	1.71	0.83	ND/MS/ MS	ND/MS/ MS	ND/MS/ MS	3.3
M5	MS	1.03	0.69	0.33	MS	MS	MS	2.0
M14	ND	ND	0.43	0.48	MS	ND	ND	0.9
M16	ND	ND	6.35	2.37	MS	MS	MS	8.7
M18	MS	1.07	1.89	ND	ND	MS	ND	3.0
M23	ND	0.56	MS	ND	ND	ND	ND	0.6
M27	ND	ND	1.19	0.15	MS	MS	MS	1.3
M30	ND	1.54	5.68	2.16	0.96	1.61	0.93	12.9
M31	ND	MS	2.21	0.86	MS	MS	MS	3.1
M32	ND	1.55	1.95	0.57	MS	MS	MS	4.1
M34	ND	MS	6.68	3.21	1.71	3.49	1.84	16.9
M35	ND	MS	2.19	1.21	ND	MS	MS	3.4
M36	ND	MS	2.74	ND	MS	MS	MS	2.7
M37	ND	MS	3.04	1.08	MS	MS	MS	4.1
Unk 3	ND	0.72	1.41	1.15	1.99	2.37	0.52	8.2
Unk 4	ND	ND	ND	0.86	ND	ND	ND	0.9
Others	ND	ND	ND	2.49	ND	ND	ND	2.5
Total	**1.06**	**11.8**	**48.3**	**20.0**	**5.49**	**8.76**	**3.99**	**99.4**

ND = not detected; MS = detected by mass spec only *M2/M17/M33 co-elute so data was reported together

[a] Metabolites including M3, M4, M7, M10, M19, M22, M24, M25, M38, M39, M40, M41, M42, M43, M44, M45 were detected by LC/MS.

DMD Fast Forward. Published on December 19, 2016 as DOI: 10.1124/dmd.116.071613
This article has not been copyedited and formatted. The final version may differ from this version.

Table 3. Molecular Ions and Characteristic Fragment Ions of Venetoclax and Metabolites in Human Plasma and/or Feces

ID	$[M+H]^+$ (Theoretical)	$[M+H]^+$ (Measured)	Δ ppm	Molecular Formula	Key Fragment Ions *(m/z)*
A-1195425	868.3254	868.3264	1.1	$C_{45}H_{51}ClN_7O_7S^+$	636.2235, 553.2363, 321.1346, 295.1553
M2	884.3203	884.3219	1.8	$C_{45}H_{51}ClN_7O_8S^+$	636.2224, 321.1349
M5	884.3203	884.3214	1.2	$C_{45}H_{51}ClN_7O_8S^+$	866.3095, 636.2225, 634.2072
M6	884.3203	884.3220	1.8	$C_{45}H_{51}ClN_7O_8S^+$	652.2177
M14	882.3046	882.3057	1.1	$C_{45}H_{49}ClN_7O_8S^+$	650.2025, 335.1135
M16	964.2771	964.2777	0.6	$C_{45}H_{51}ClN_7O_{11}S_2^+$	884.3198, 636.2230, 569.2311, 321.1345
M17	900.3152	900.3185	3.7	$C_{45}H_{51}ClN_7O_9S^+$	668.2135, 321.1346
M18	898.2996	898.3020	2.7	$C_{45}H_{49}ClN_7O_9S^+$	636.2232, 321.1346
M23	916.3101	916.3124	2.5	$C_{45}H_{51}ClN_7O_{10}S^+$	898.2997
M27	882.3046	882.3042	-0.5	$C_{45}H_{49}ClN_7O_8S^+$	864.2936, 634.2056, 567.2184
M30	838.3512	838.3519	0.9	$C_{45}H_{53}ClN_7O_5S^+$	606.2493, 321.1347
M31	854.3461	854.3466	0.6	$C_{45}H_{53}ClN_7O_6S^+$	606.2488, 569.2312, 321.1345, 295.1550
M32	854.3461	854.3464	0.3	$C_{45}H_{53}ClN_7O_6S^+$	836.3355, 606.2484
M33	854.3461	854.3464	0.4	$C_{45}H_{53}ClN_7O_6S^+$	836.3354, 606.2489, 604.2334
M34	934.3029	934.3040	1.1	$C_{45}H_{53}ClN_7O_9S_2^+$	854.3462, 606.2491, 569.2313, 321.1347
M35	854.3461	854.3464	0.4	$C_{45}H_{53}ClN_7O_6S^+$	937.3220, 606.2492, 569.2314, 321.1347
M36	870.3410	870.3415	0.5	$C_{45}H_{53}ClN_7O_7S^+$	852.3302, 606.2489
M37	870.3410	870.3416	0.6	$C_{45}H_{53}ClN_7O_7S^+$	852.3302, 606.2489

DMD Fast Forward. Published on December 19, 2016 as DOI: 10.1124/dmd.116.071613
This article has not been copyedited and formatted. The final version may differ from this version.

Figure 1

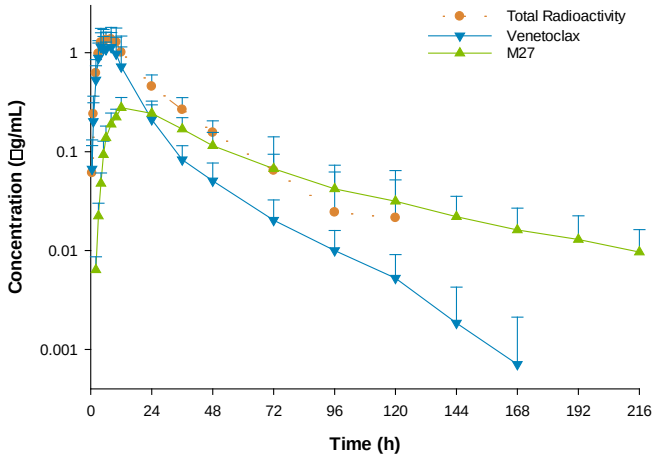

Total radioactivity is expressed as microgram-equivalents/gram (µg-eq/g).

DMD Fast Forward. Published on December 19, 2016 as DOI: 10.1124/dmd.116.071613
This article has not been copyedited and formatted. The final version may differ from this version.

Figure 2

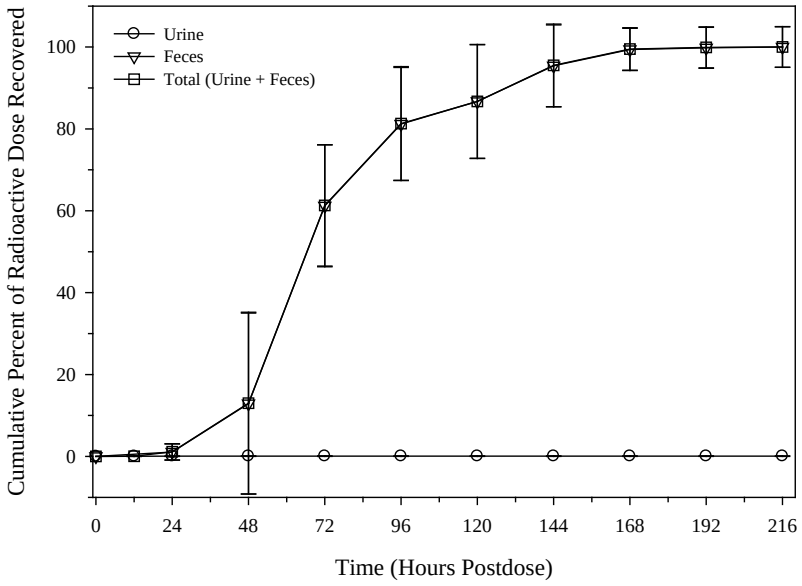

DMD Fast Forward. Published on December 19, 2016 as DOI: 10.1124/dmd.116.071613
This article has not been copyedited and formatted. The final version may differ from this version.

Figure 3

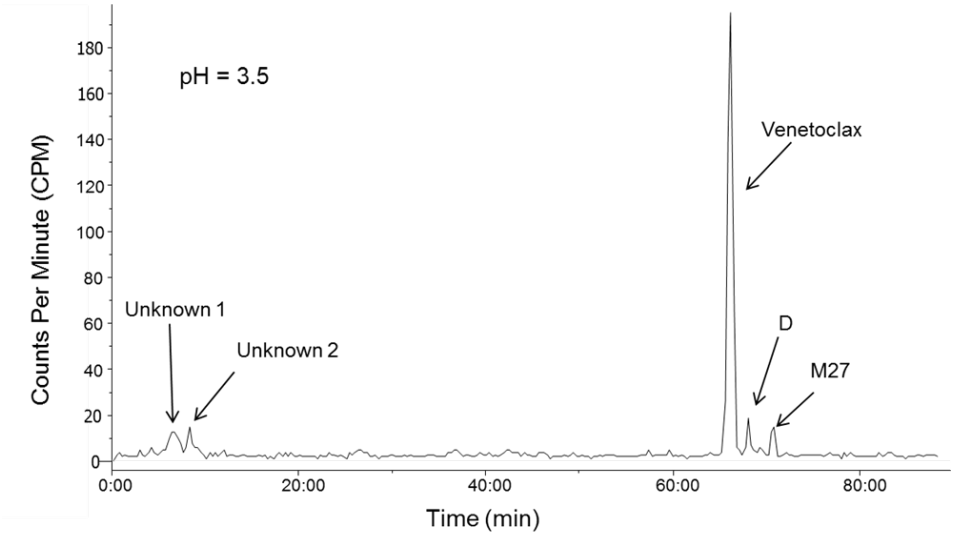

D: on-column degradation product of M27

DMD Fast Forward. Published on December 19, 2016 as DOI: 10.1124/dmd.116.071613
This article has not been copyedited and formatted. The final version may differ from this version.

Figure 4

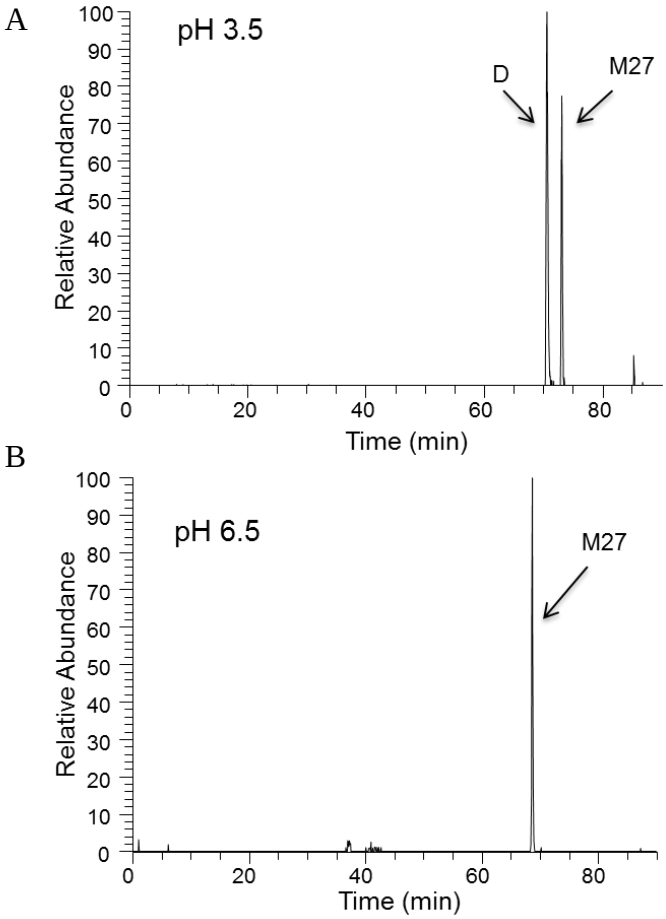

DMD Fast Forward. Published on December 19, 2016 as DOI: 10.1124/dmd.116.071613
This article has not been copyedited and formatted. The final version may differ from this version.

Figure 5

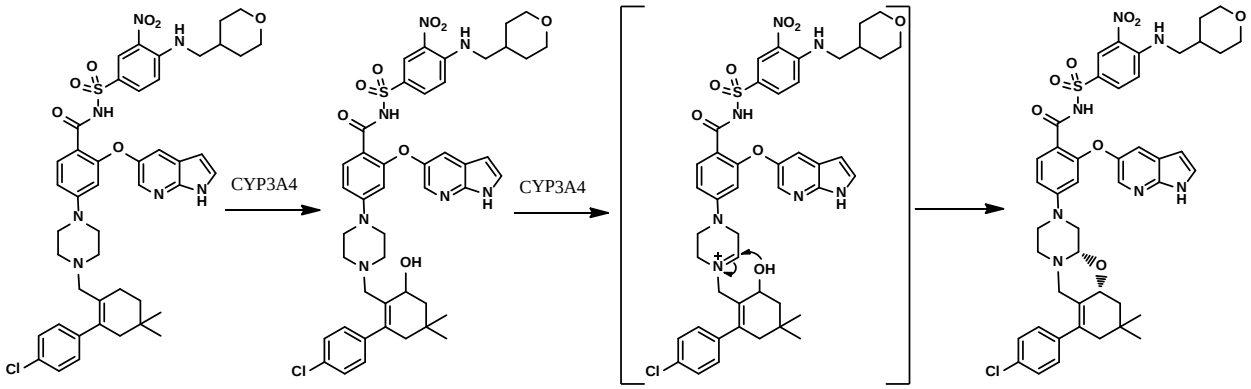

Venetoclax M5 M27

DMD Fast Forward. Published on December 19, 2016 as DOI: 10.1124/dmd.116.071613
This article has not been copyedited and formatted. The final version may differ from this version.

Figure 6

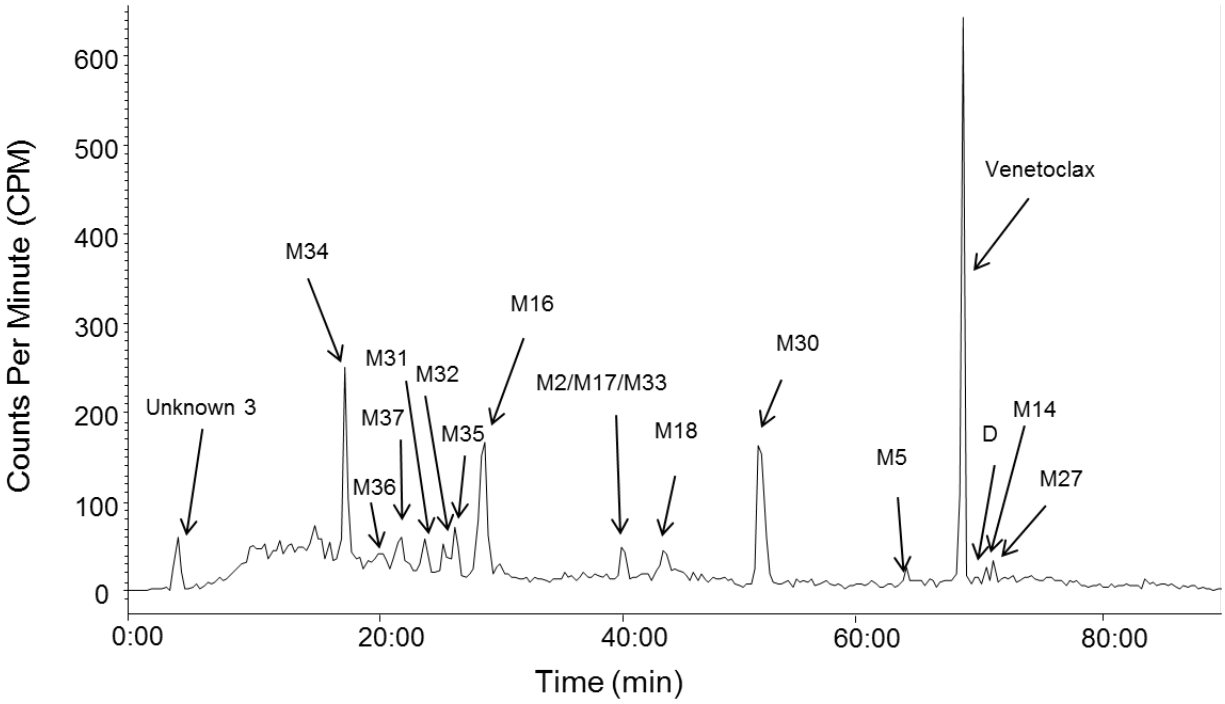

D: on-column degradation product of M27

DMD Fast Forward. Published on December 19, 2016 as DOI: 10.1124/dmd.116.071613
This article has not been copyedited and formatted. The final version may differ from this version.

Figure 7

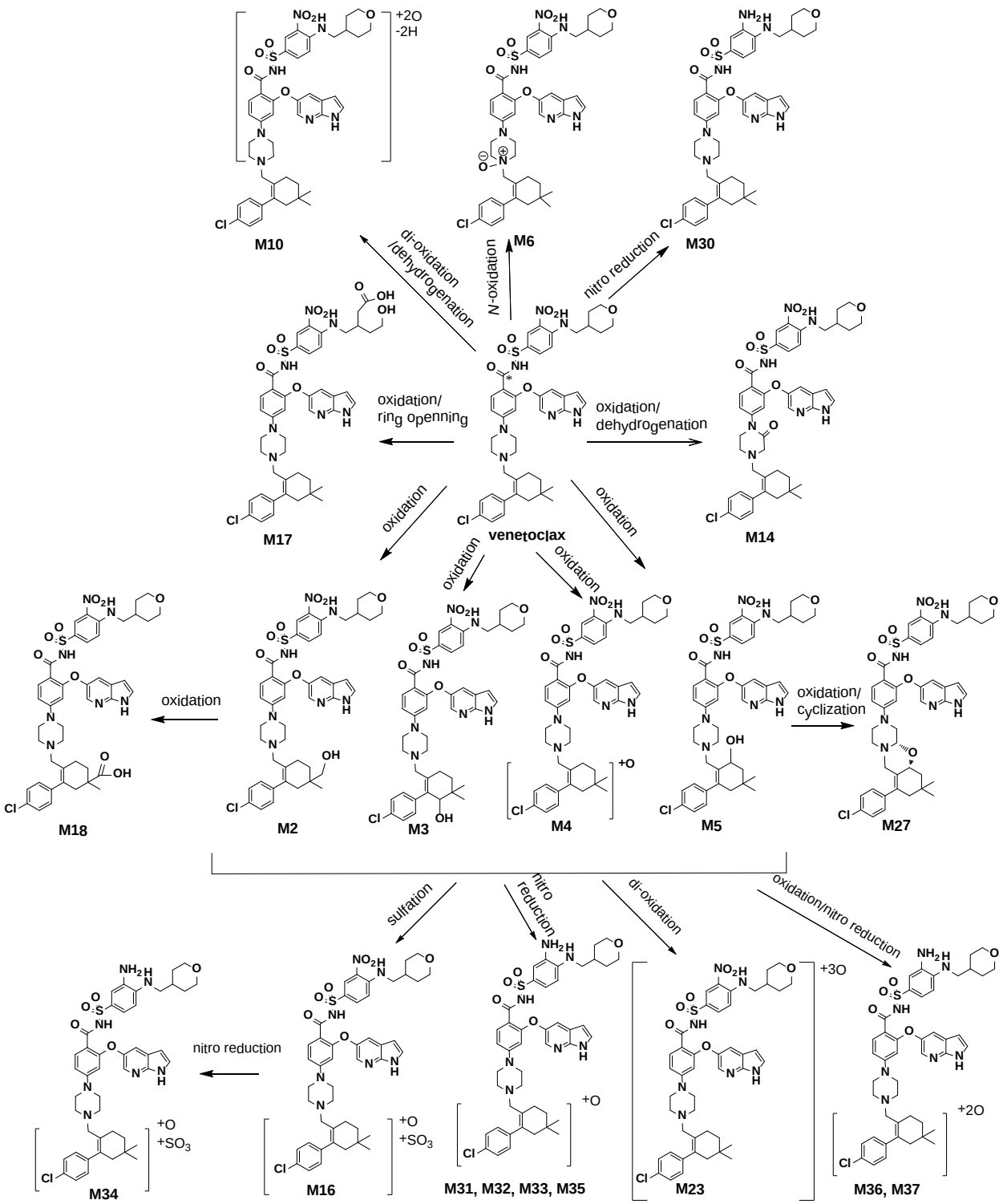

Asterisk denotes position of [^{14}C]venetoclax.

M7, M19, M22, M24, M25, M38-M45 not shown as they were detected in fecal samples by LC/MS only.

DMD Fast Forward. Published on December 19, 2016 as DOI: 10.1124/dmd.116.071613
This article has not been copyedited and formatted. The final version may differ from this version.

Figure 8

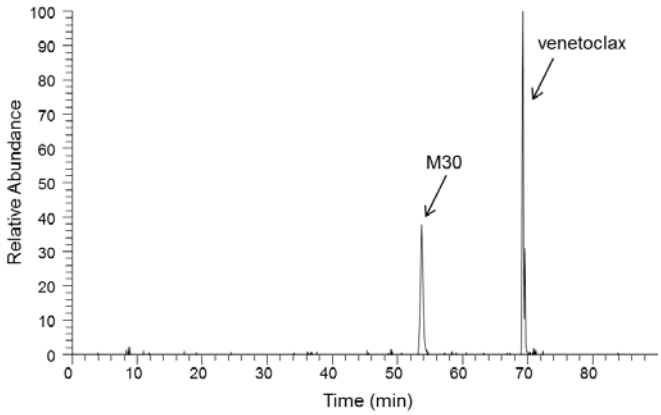

Title: Metabolism and Disposition of a Novel Bcl-2 Inhibitor Venetoclax in Humans and Characterization of its Unusual Metabolites

Authors: Hong Liu, Melissa J. Michmerhuizen, Yanbin Lao, Katty Wan, Ahmed Hamed Salem, James Sawicki, Michael Serby, Srirajan Vaidyanathan, Shekman L. Wong, Suresh Agarwal, Martin Dunbar, Jens Sydor, Sonia M. de Morais, Anthony J. Lee

Bioanalysis and Biotransformation, Research & Development, AbbVie, North Chicago, Illinois (H.L., M.J.M., K.W., J.S., M.S., J.S., S.M.M., A.J.L.); Process Chemistry, AbbVie, North Chicago, Illinois (S.V.); Clinical Pharmacology and Pharmacometrics, AbbVie, North Chicago, Illinois (A.H.S., S.L.W., S.A., M.D.); Clinical Pharmacy, Faculty of Pharmacy, Ain Shams University, Cairo, Egypt (A.H.S.); Eli Lilly and Company, Indianapolis, IN (Y.L.)

Drug Metabolism and Disposition

Supplemental Figures

Supplemental Tables

Supplemental Figure 1

Venetoclax

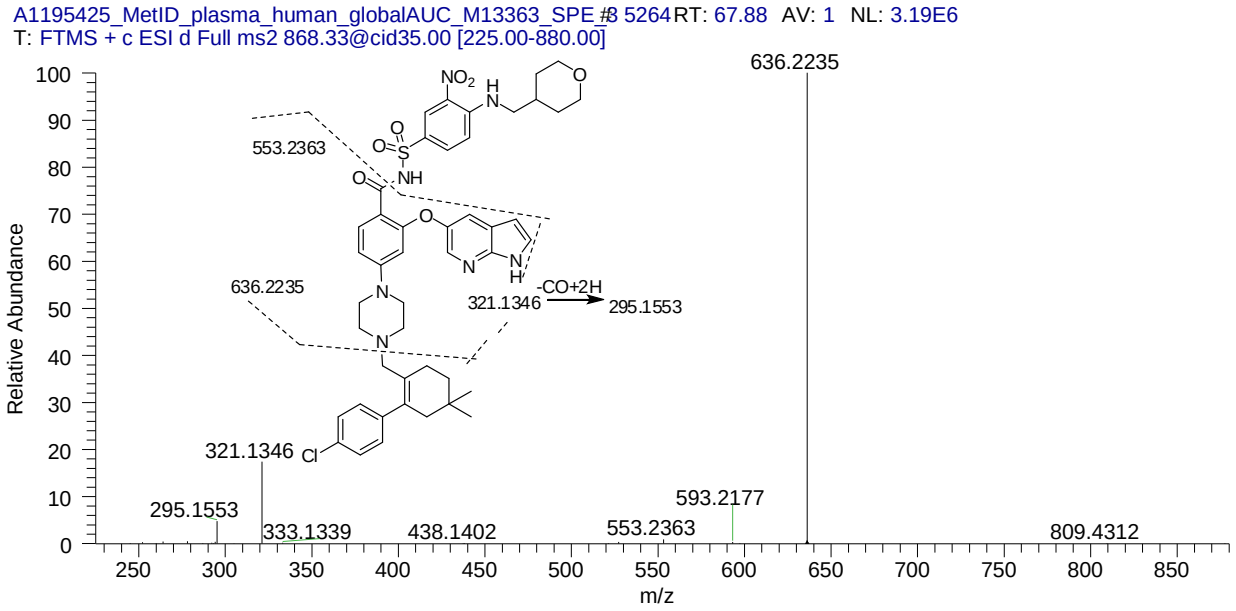

M2

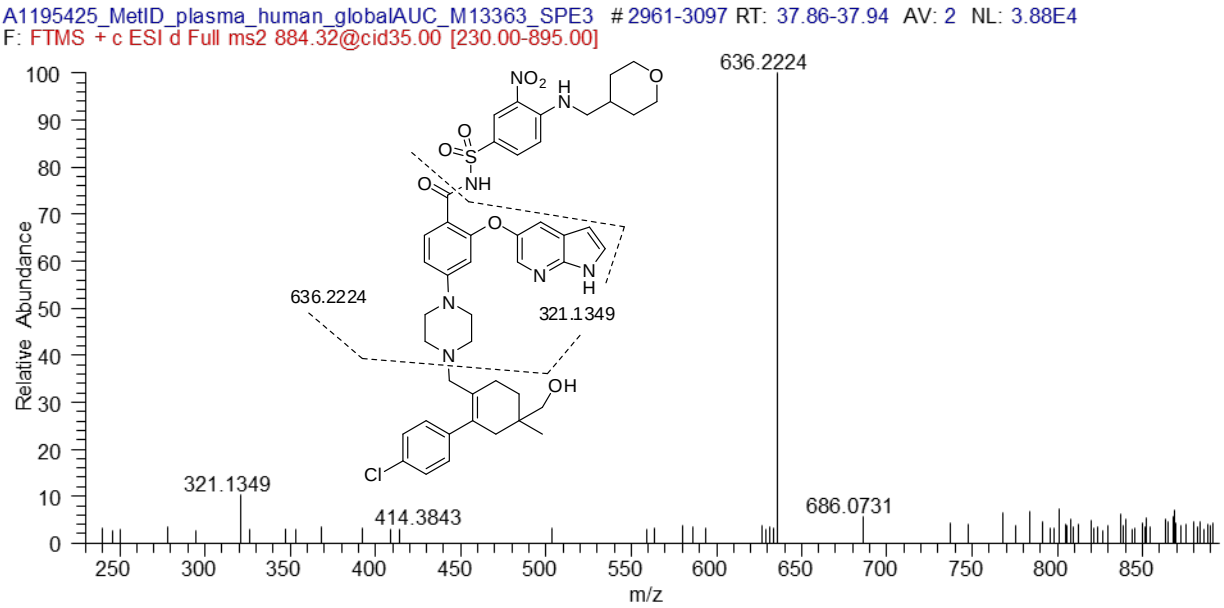

M5

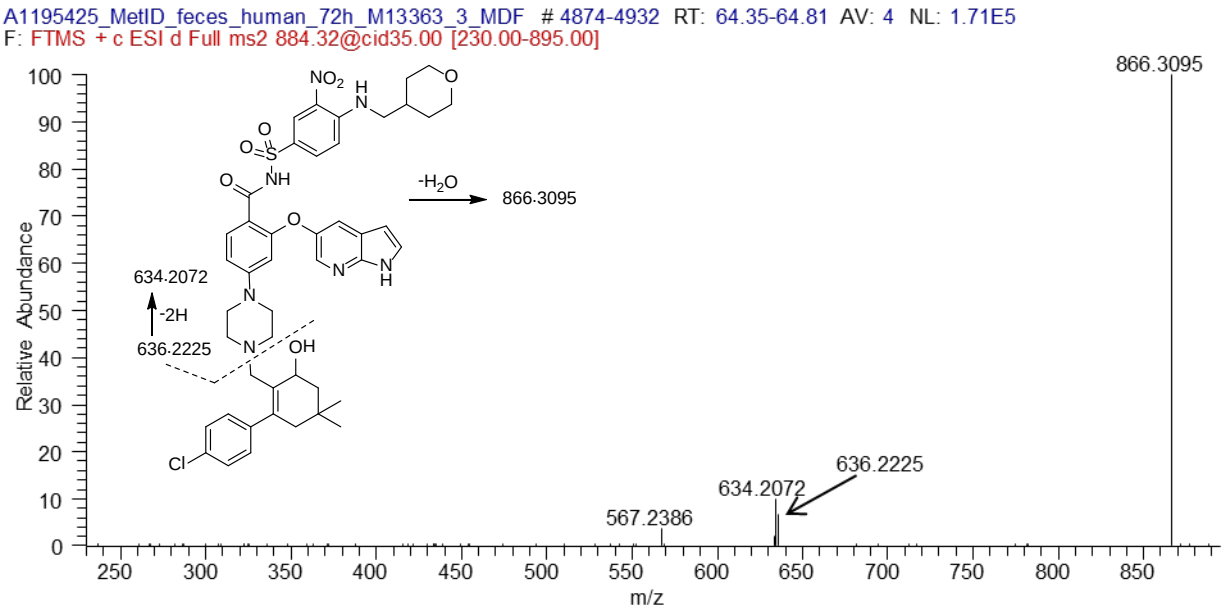
A1195425_MetID_feces_human_72h_M13363_3_MDF # 4874-4932 RT: 64.35-64.81 AV: 4 NL: 1.71E5
F: FTMS + c ESI d Full ms2 884.32@cid35.00 [230.00-895.00]
866.3095
-H2O
866.3095
634.2072
-2H
636.2225
636.2225
634.2072
567.2386
Relative Abundance
m/z

M6

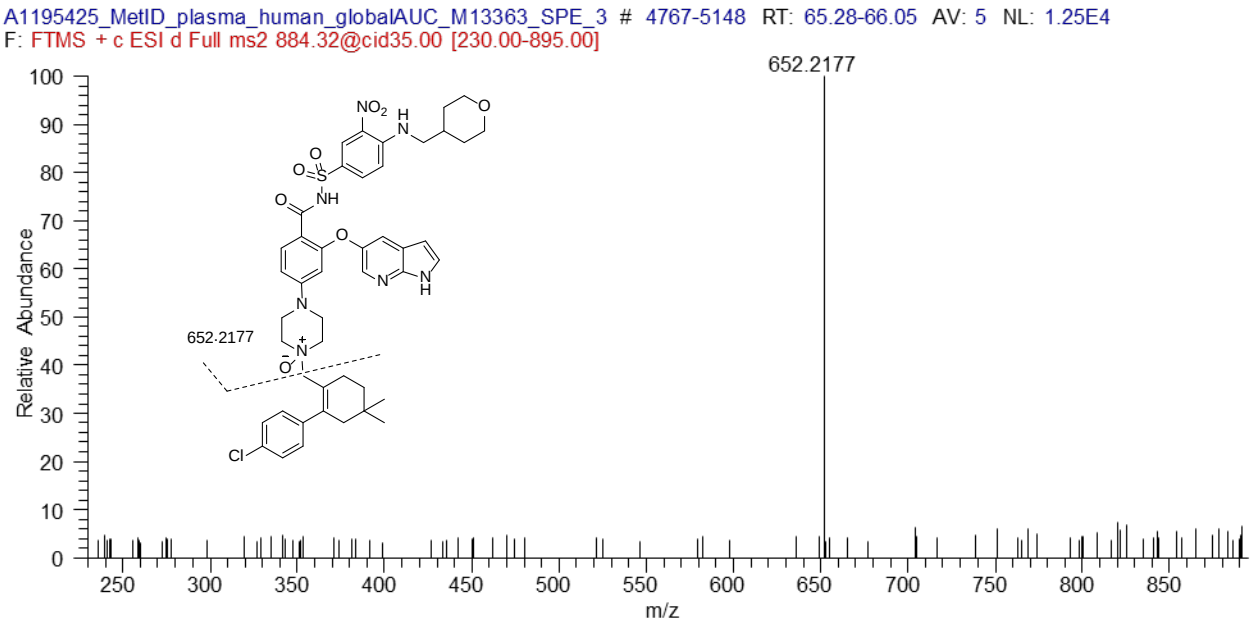
A1195425_MetID_plasma_human_globalAUC_M13363_SPE_3 # 4767-5148 RT: 65.28-66.05 AV: 5 NL: 1.25E4
F: FTMS + c ESI d Full ms2 884.32@cid35.00 [230.00-895.00]
652.2177
652.2177
Relative Abundance
m/z

M16

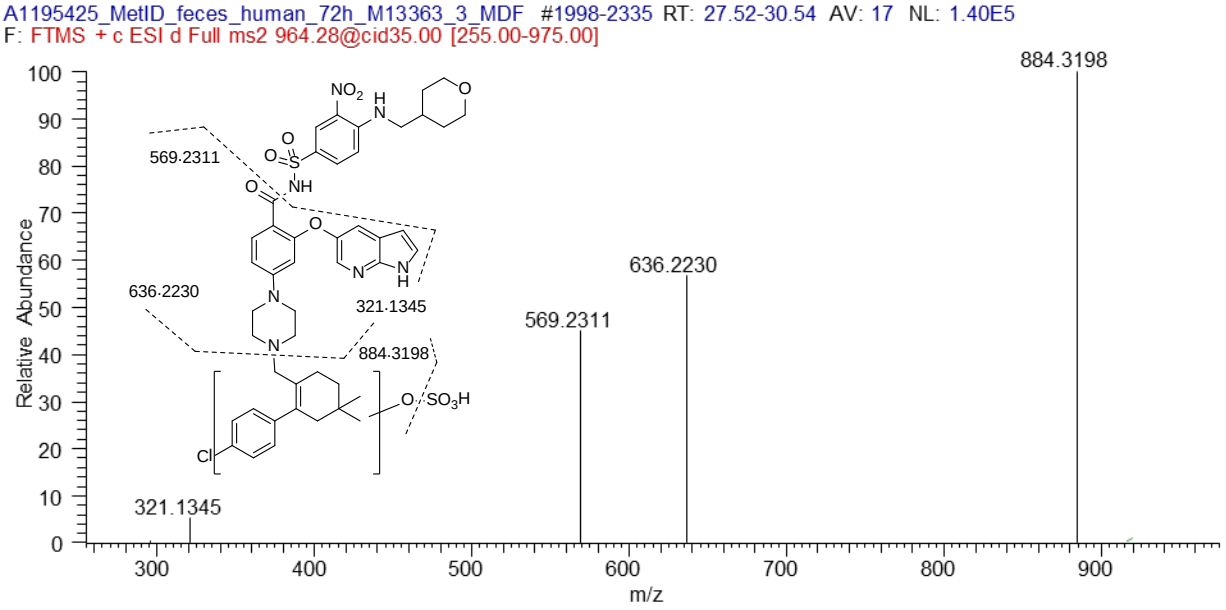
A1195425_MetID_feces_human_72h_M13363_3_MDF #1998-2335 RT: 27.52-30.54 AV: 17 NL: 1.40E5
F: FTMS + c ESI d Full ms2 964.28@cid35.00 [255.00-975.00]
884.3198
636.2230
569.2311
321.1345
Relative Abundance
m/z

M17

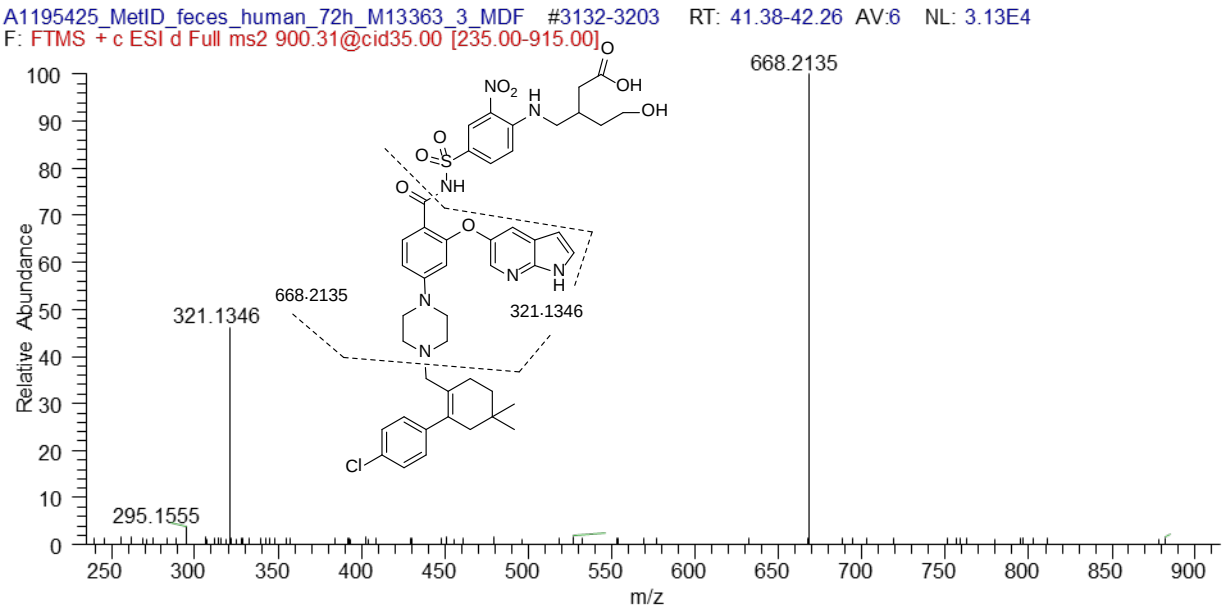
A1195425_MetID_feces_human_72h_M13363_3_MDF #3132-3203 RT: 41.38-42.26 AV:6 NL: 3.13E4
F: FTMS + c ESI d Full ms2 900.31@cid35.00 [235.00-915.00]
668.2135
321.1346
295.1555
Relative Abundance
m/z

M18

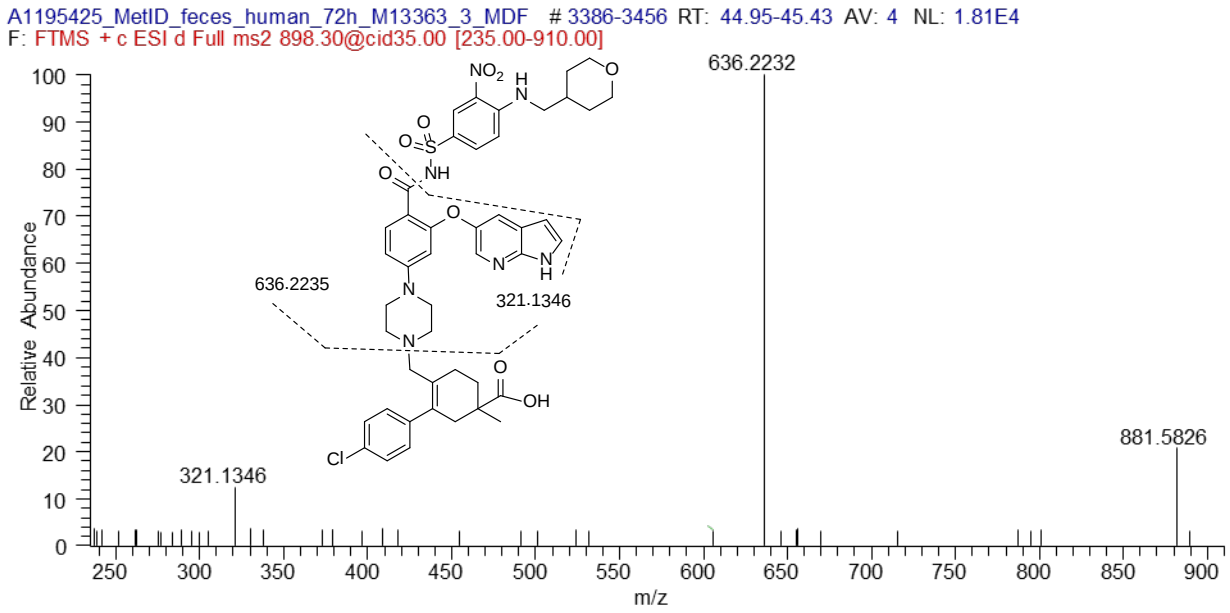
A1195425_MetID_feces_human_72h_M13363_3_MDF # 3386-3456 RT: 44.95-45.43 AV: 4 NL: 1.81E4
F: FTMS + c ESI d Full ms2 898.30@cid35.00 [235.00-910.00]
636.2232
636.2235
321.1346
881.5826
321.1346
Relative Abundance
m/z

M27

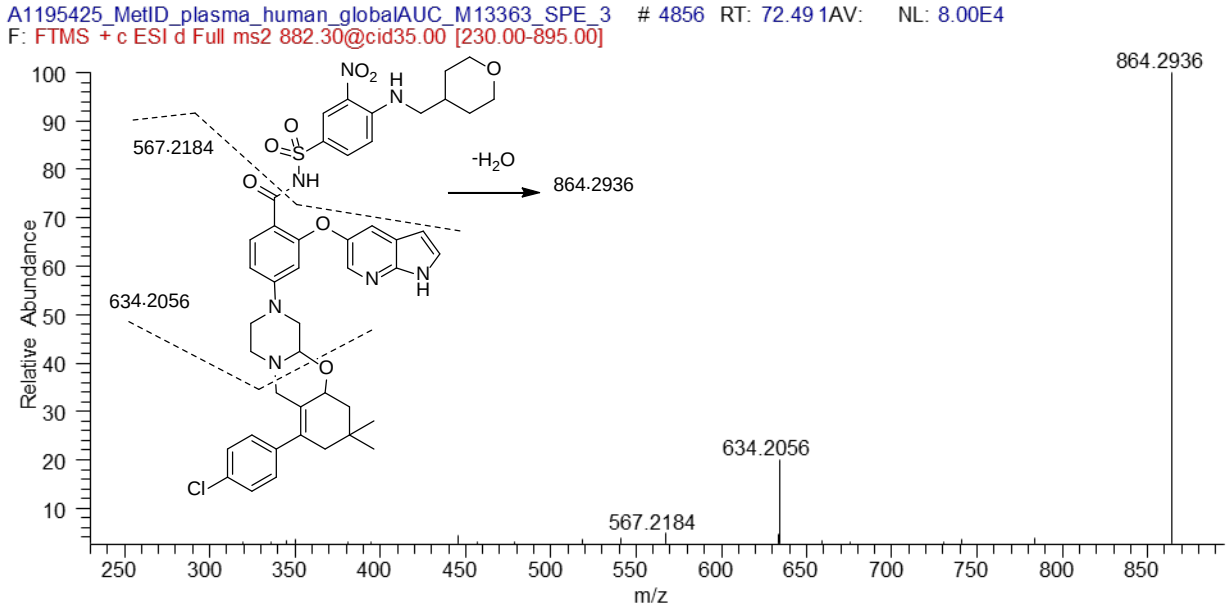
A1195425_MetID_plasma_human_globalAUC_M13363_SPE_3 # 4856 RT: 72.49 1AV: NL: 8.00E4
F: FTMS + c ESI d Full ms2 882.30@cid35.00 [230.00-895.00]
864.2936
567.2184
-H2O
864.2936
634.2056
634.2056
567.2184
Relative Abundance
m/z

M30

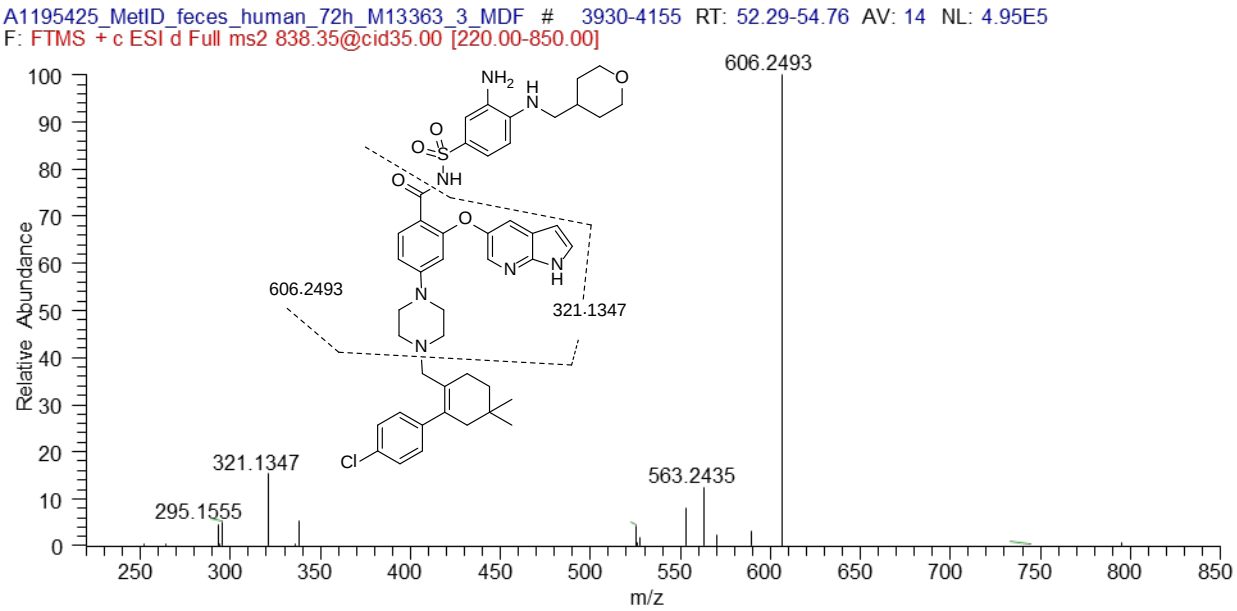
A1195425_MetID_feces_human_72h_M13363_3_MDF # 3930-4155 RT: 52.29-54.76 AV: 14 NL: 4.95E5
F: FTMS + c ESI d Full ms2 838.35@cid35.00 [220.00-850.00]
606.2493
606.2493
321.1347
321.1347
563.2435
295.1555
Relative Abundance
m/z

M31

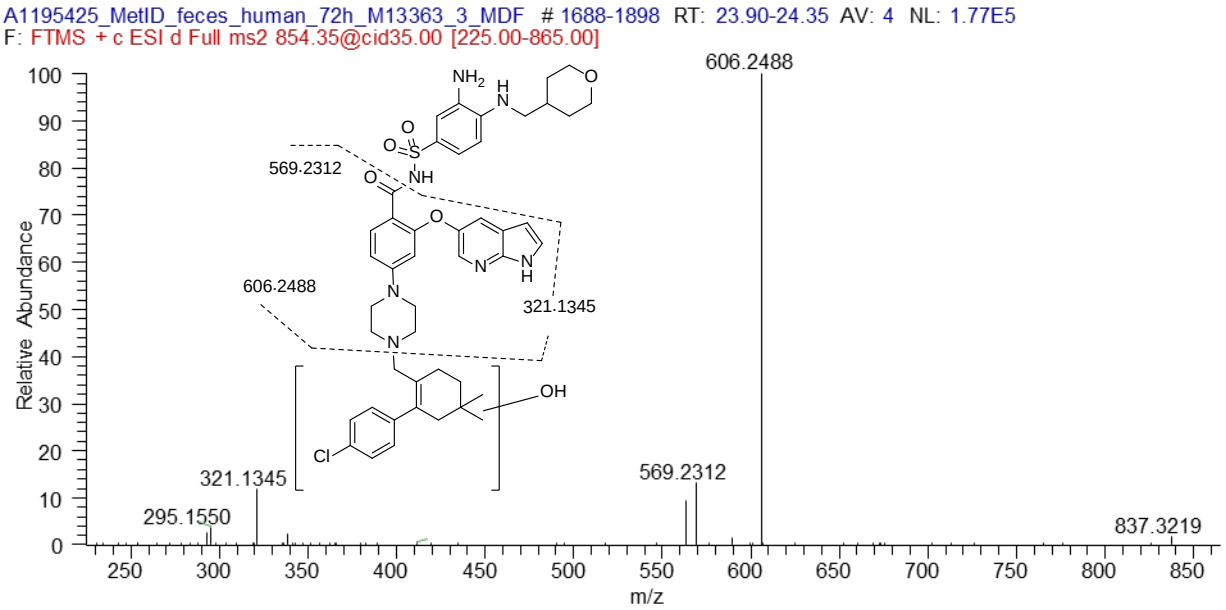
A1195425_MetID_feces_human_72h_M13363_3_MDF # 1688-1898 RT: 23.90-24.35 AV: 4 NL: 1.77E5
F: FTMS + c ESI d Full ms2 854.35@cid35.00 [225.00-865.00]
606.2488
569.2312
606.2488
321.1345
321.1345
569.2312
295.1550
837.3219
Relative Abundance
m/z

M32

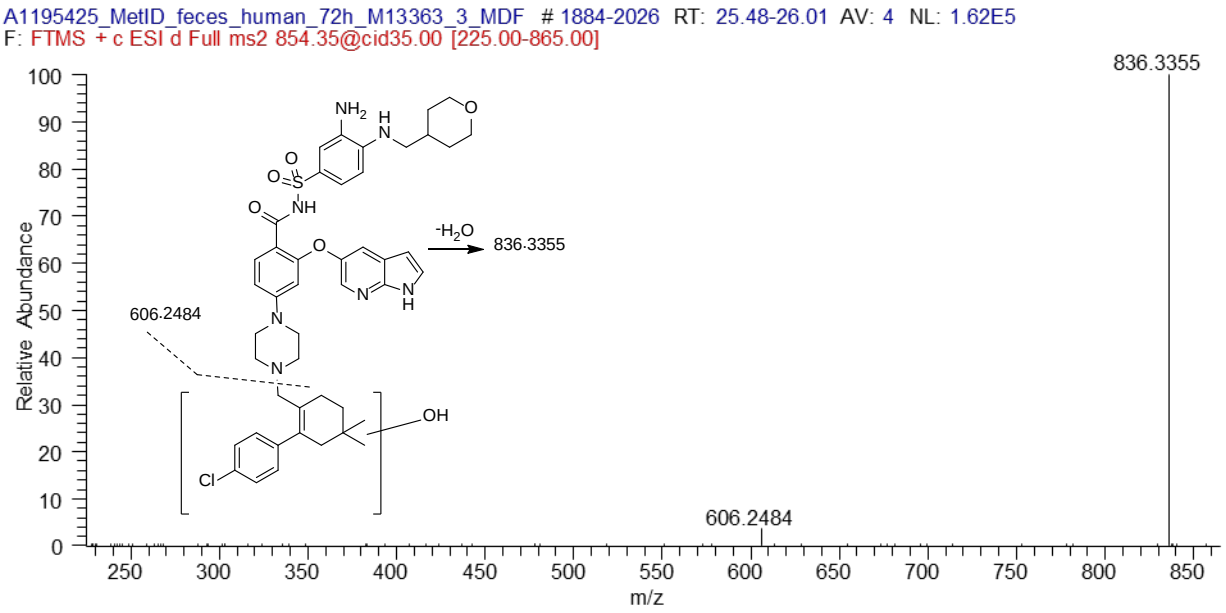
A1195425_MetID_feces_human_72h_M13363_3_MDF # 1884-2026 RT: 25.48-26.01 AV: 4 NL: 1.62E5
F: FTMS + c ESI d Full ms2 854.35@cid35.00 [225.00-865.00]
836.3355
606.2484
-H2O
836.3355
606.2484
OH
Cl
Relative Abundance
m/z

M33

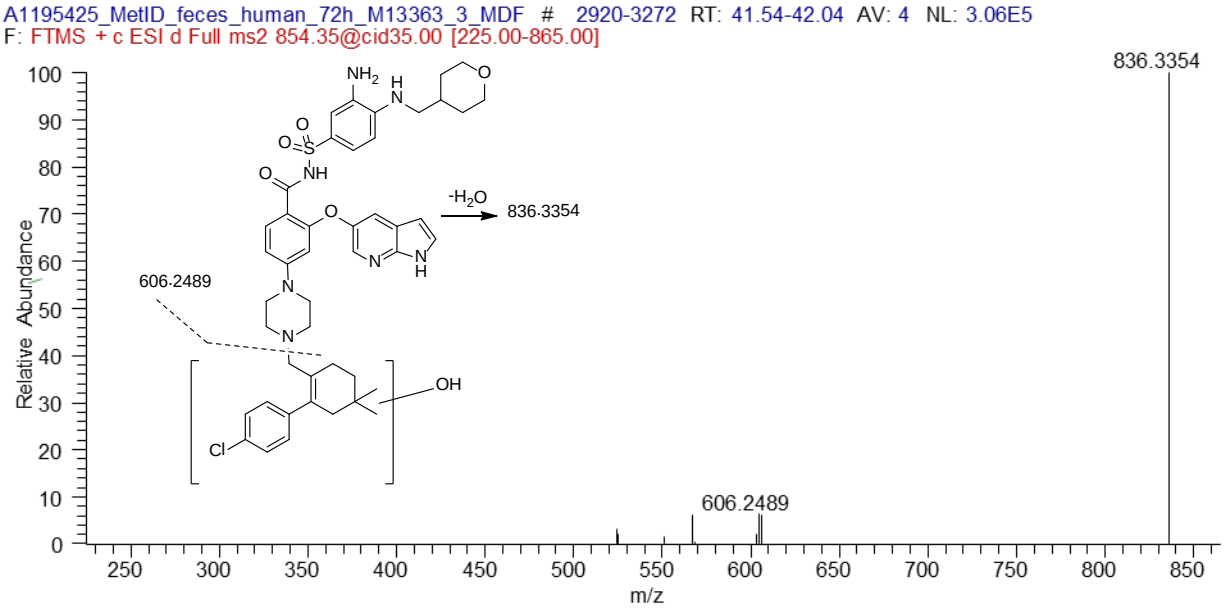
A1195425_MetID_feces_human_72h_M13363_3_MDF # 2920-3272 RT: 41.54-42.04 AV: 4 NL: 3.06E5
F: FTMS + c ESI d Full ms2 854.35@cid35.00 [225.00-865.00]
836.3354
606.2489
-H2O
836.3354
606.2489
OH
Cl
Relative Abundance
m/z

M34

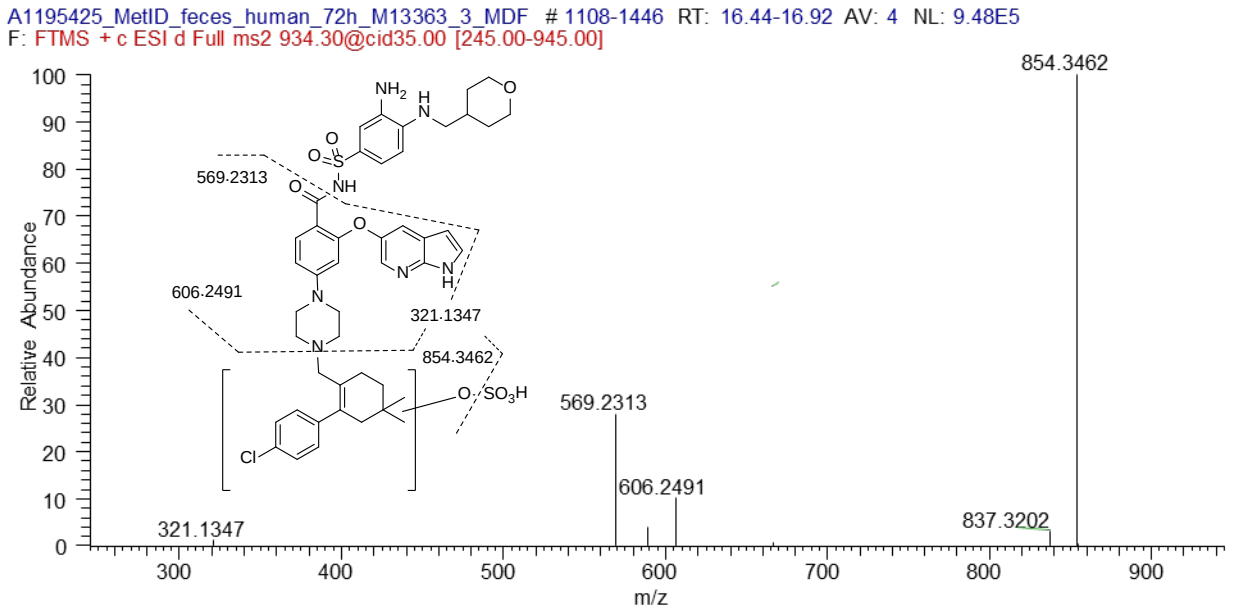
A1195425_MetID_feces_human_72h_M13363_3_MDF # 1108-1446 RT: 16.44-16.92 AV: 4 NL: 9.48E5
F: FTMS + c ESI d Full ms2 934.30@cid35.00 [245.00-945.00]
Relative Abundance
m/z
854.3462
569.2313
606.2491
321.1347
837.3202
569.2313
606.2491
321.1347
854.3462

M35

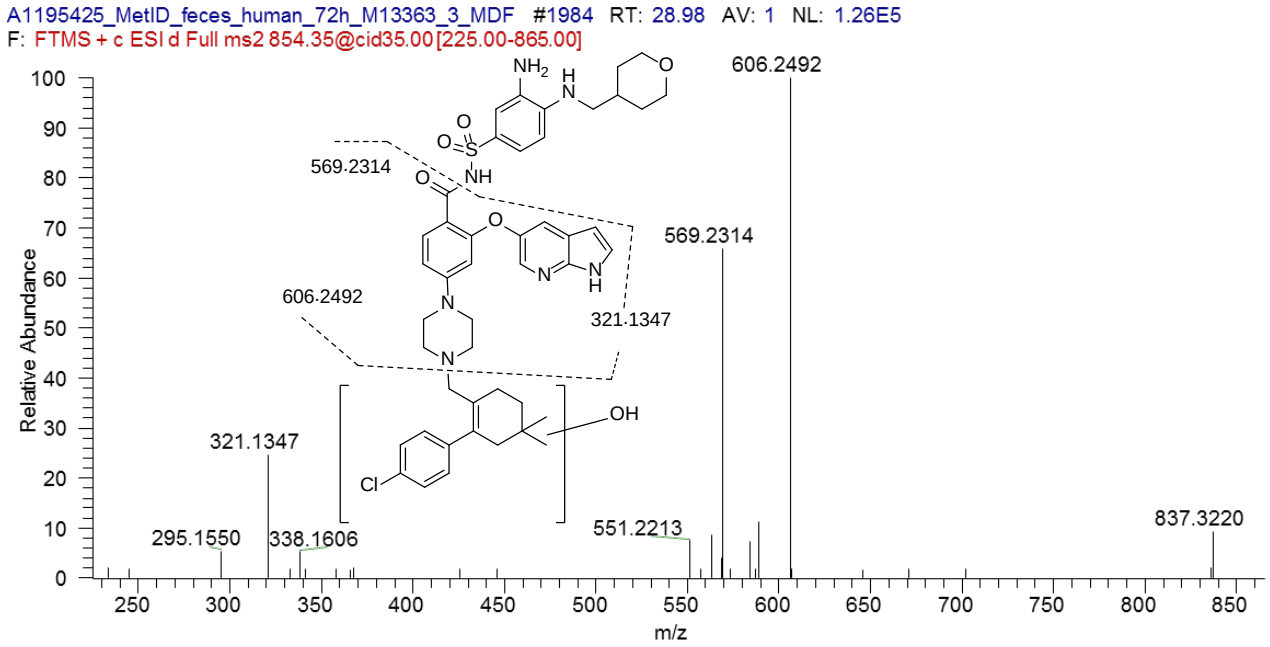
A1195425_MetID_feces_human_72h_M13363_3_MDF #1984 RT: 28.98 AV: 1 NL: 1.26E5
F: FTMS + c ESI d Full ms2 854.35@cid35.00 [225.00-865.00]
Relative Abundance
m/z
606.2492
569.2314
569.2314
606.2492
321.1347
321.1347
295.1550
338.1606
551.2213
837.3220

M36

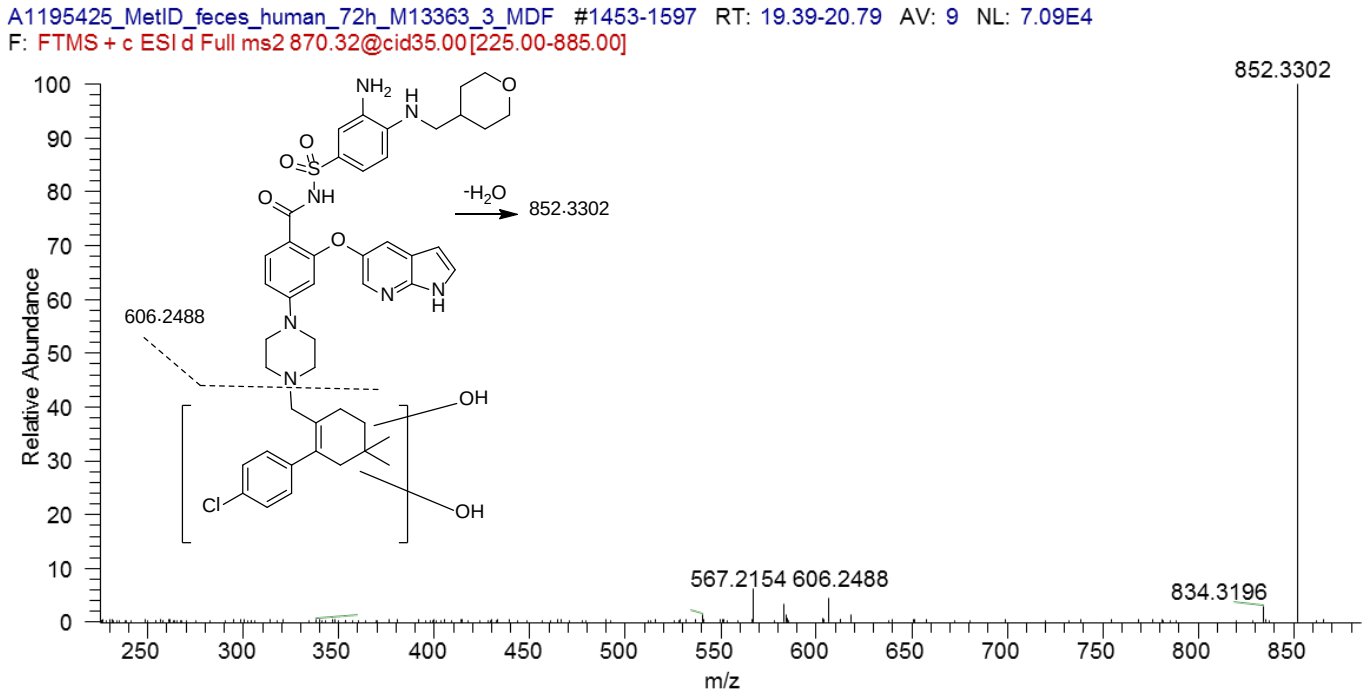
A1195425_MetID_feces_human_72h_M13363_3_MDF #1453-1597 RT: 19.39-20.79 AV: 9 NL: 7.09E4
F: FTMS + c ESI d Full ms2 870.32@cid35.00 [225.00-885.00]
852.3302
-H2O
852.3302
606.2488
567.2154 606.2488
834.3196
Relative Abundance
m/z

M37

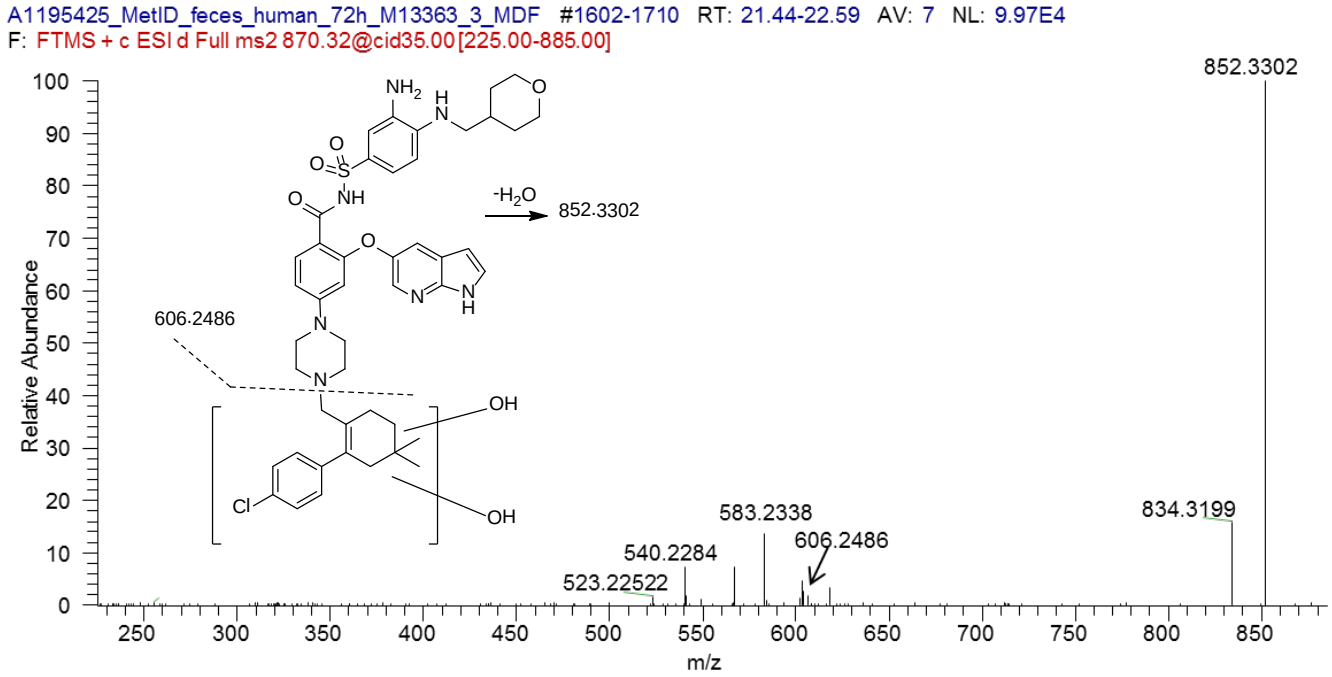
A1195425_MetID_feces_human_72h_M13363_3_MDF #1602-1710 RT: 21.44-22.59 AV: 7 NL: 9.97E4
F: FTMS + c ESI d Full ms2 870.32@cid35.00 [225.00-885.00]
852.3302
-H2O
852.3302
606.2486
583.2338
606.2486
540.2284
523.22522
834.3199
Relative Abundance
m/z

Supplemental Figure 2.

(A)

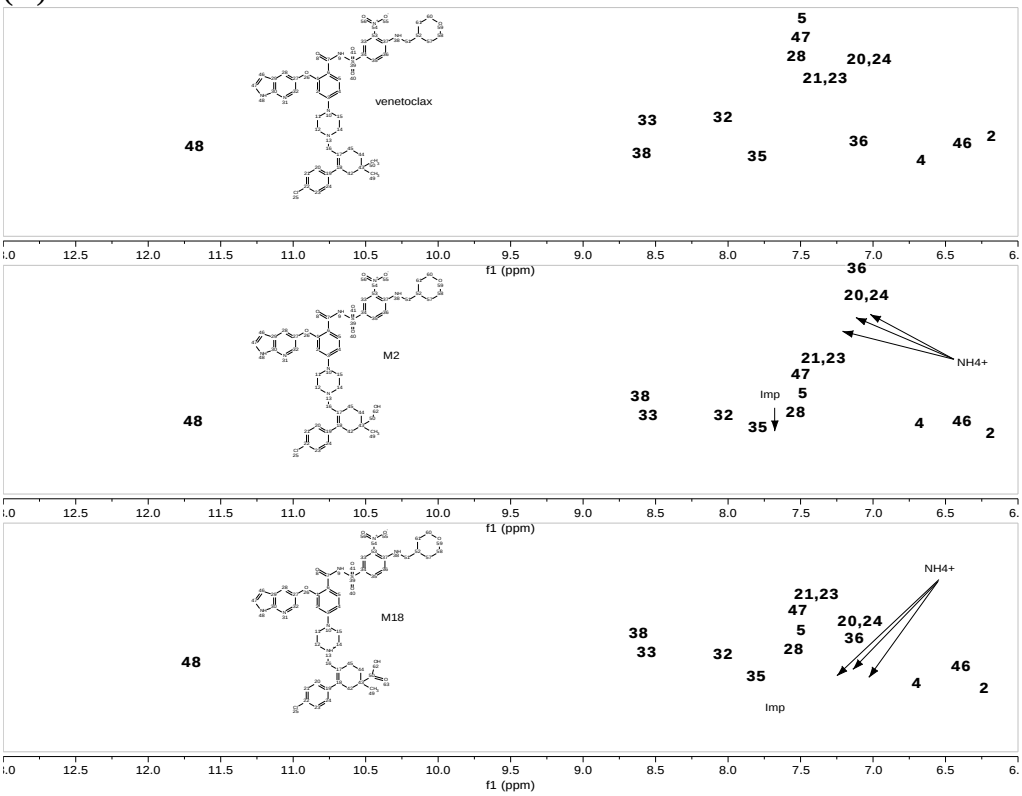

(B)

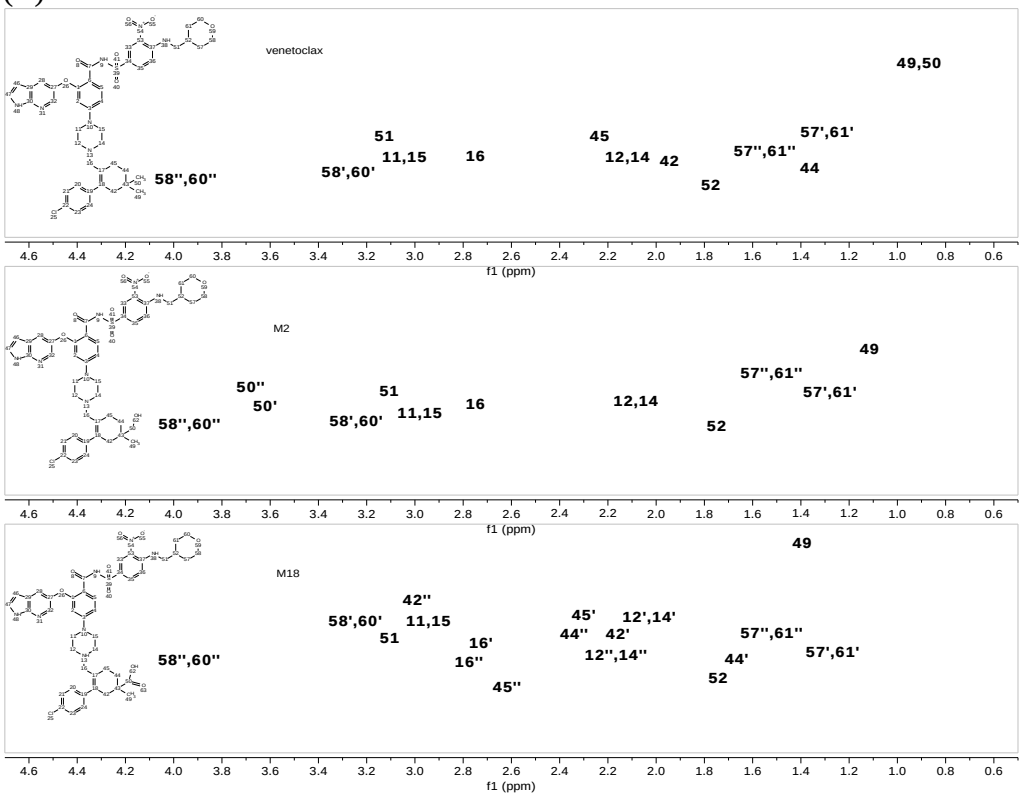

Supplemental Figure 3

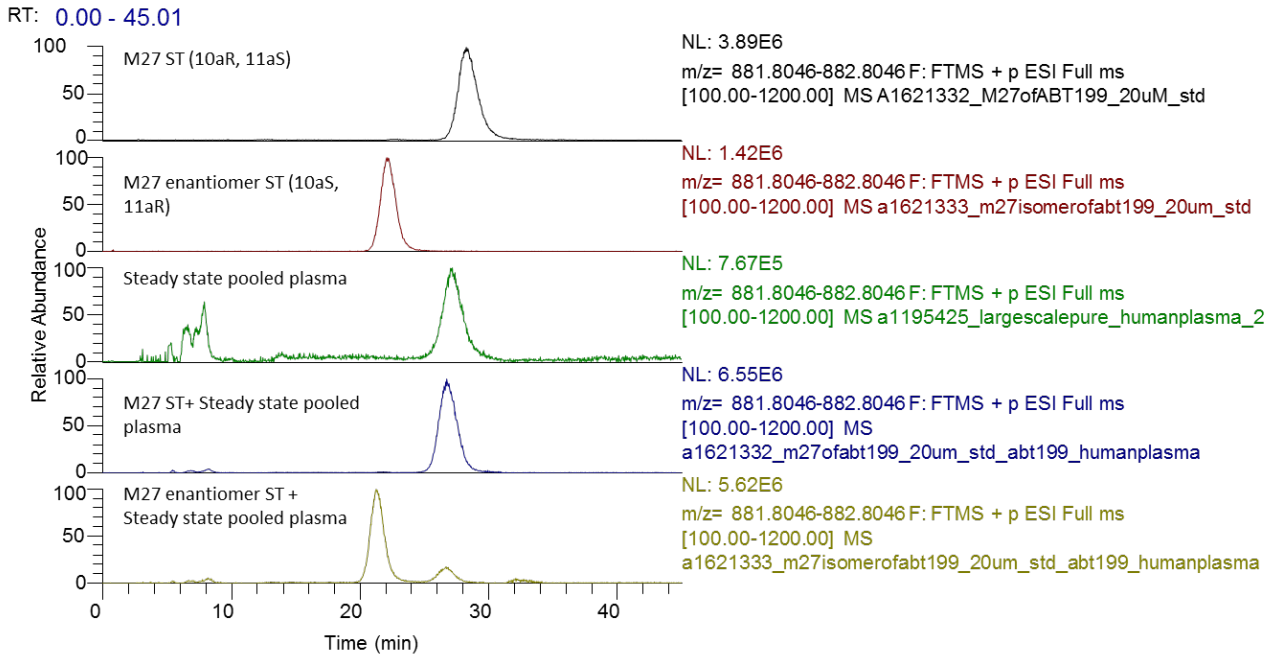

ST: synthetic standard; The chromatographic separation of M27 and M27 enantiomer was achieved at room temperature on an chiral Pak IC3, 3 µm, 4.6 x 250 mm HPLC column. Mobile phases were A: 25 mM ammonium biocarbonate (45%) and B: 100% acetonitrile (55%). The flow rate was maintained at 1.0 mL/min.

Supplemental Figure 4

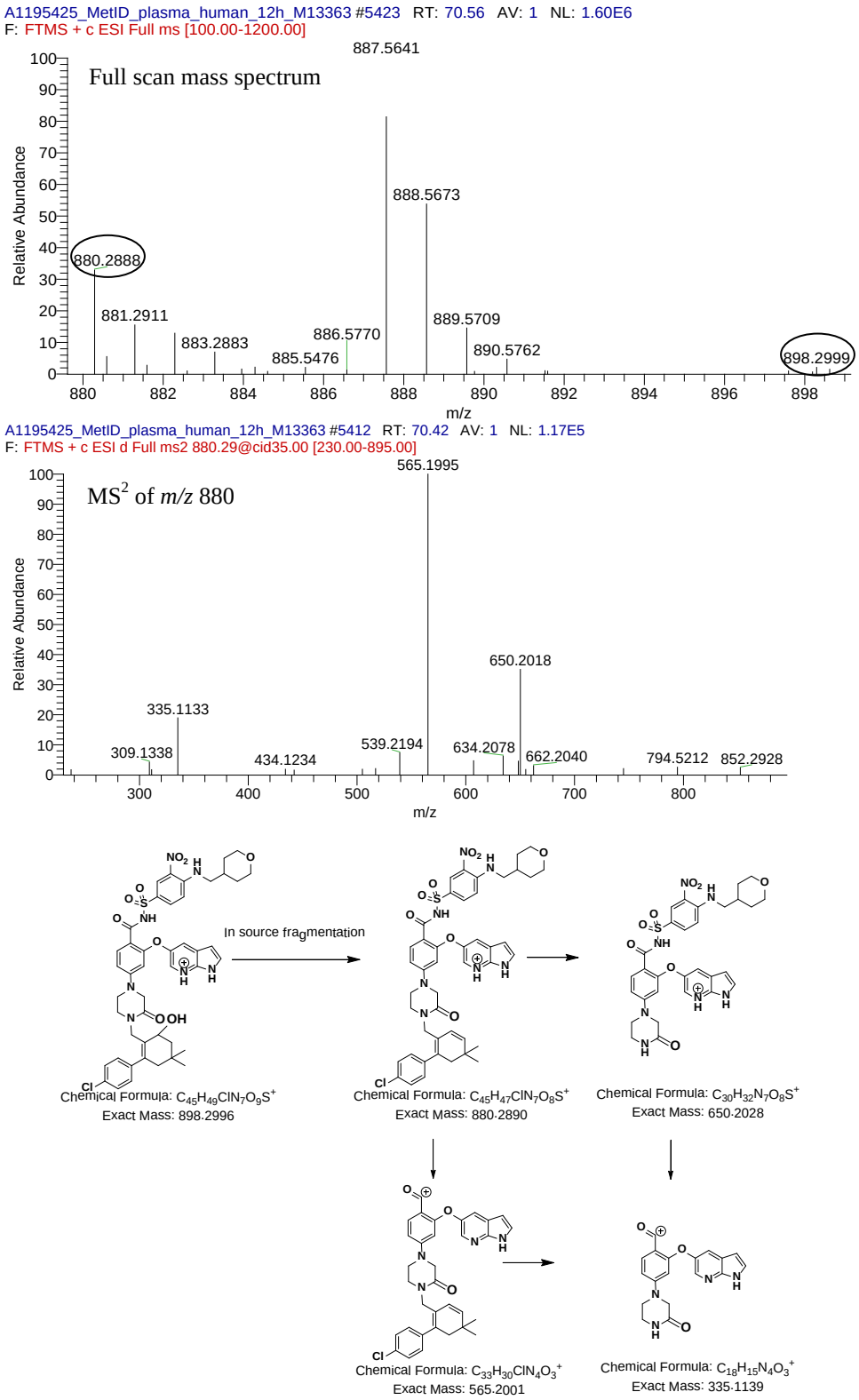

Sites of protonation are randomly assigned for the ions at m/z 898.2996, 880.2890, and 650.2028.

Supplemental Figure 5

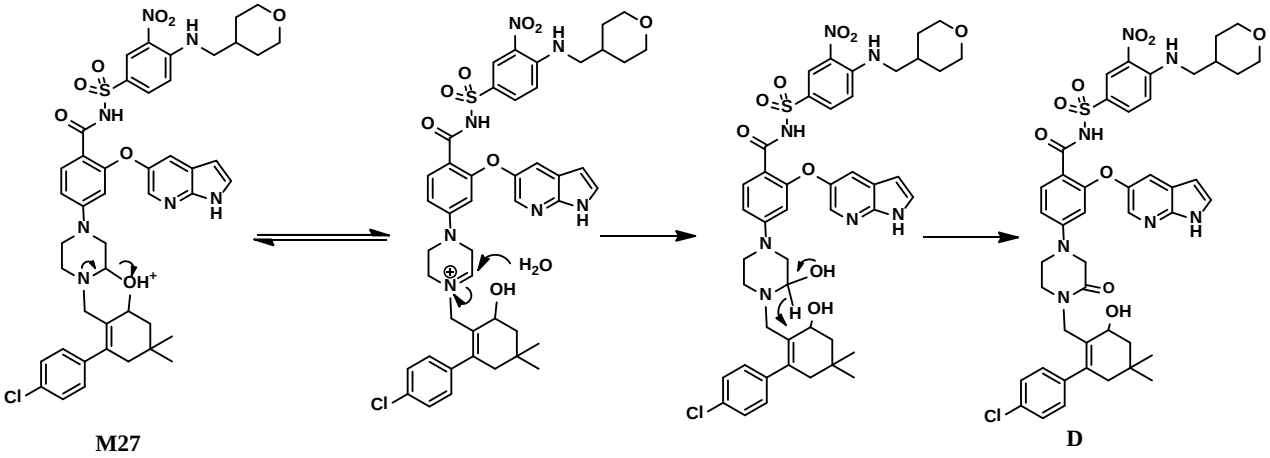

Supplemental Table 1

ID	$[M+H]^+$ (Theoretical)	$[M+H]^+$ (Measured)	Δ ppm	Molecular Formula	Key Fragment Ions *(m/z)*
M3	884.3203	884.3222	2.1	$C_{45}H_{51}ClN_7O_8S^+$	866.3117, 636.2267
M4	884.3203	884.3220	1.8	$C_{45}H_{51}ClN_7O_8S^+$	636.2229, 321.1343
M7	842.3097	842.3096	-0.2	$C_{43}H_{49}ClN_7O_7S^+$	610.2073
M10	898.2996	898.3007	0.3	$C_{45}H_{49}ClN_7O_9S^+$	666.2003
M19	916.3101	916.3106	0.5	$C_{45}H_{51}ClN_7O_{10}S^+$	898.3000, 668.2128, 321.1343
M22	900.3152	900.3173	2.3	$C_{45}H_{51}ClN_7O_9S^+$	882.3047
M24	900.3152	900.3159	0.8	$C_{45}H_{51}ClN_7O_9S^+$	882.3050, 864.2951
M25	900.3152	900.3158	0.7	$C_{45}H_{51}ClN_7O_9S^+$	882.3047
M38	900.3152	900.3179	3.0	$C_{45}H_{51}ClN_7O_9S^+$	882.3025, 668.2057, 321.1333
M39	916.3101	916.3063	-4.1	$C_{45}H_{51}ClN_7O_{10}S^+$	898.2992
M40	916.3101	916.3115	1.5	$C_{45}H_{51}ClN_7O_{10}S^+$	668.2129, 321.1344
M41	916.3101	916.3131	3.3	$C_{45}H_{51}ClN_7O_{10}S^+$	668.2119
M42	916.3101	916.3123	2.3	$C_{45}H_{51}ClN_7O_{10}S^+$	668.2110
M43	870.3410	870.3414	0.4	$C_{45}H_{53}ClN_7O_7S^+$	852.3307, 638.2371, 553.2358
M44	570.2630	570.2632	0.3	$C_{33}H_{37}ClN_5O_2^+$	338.1611, 321.1343
M45	868.3254	868.3255	0.1	$C_{45}H_{51}ClN_7O_7S^+$	606.2484, 583.2104, 321.1345

M3. M3 was detected in plasma and feces with a protonated molecular ion of *m/z* 884.3222. Measured accurate mass data suggested the molecular formula of $C_{45}H_{51}ClN_7O_8S^+$. Collision-

induced dissociation of M3 generated fragment ions at *m/z* 866.3117 and 636.2267, suggesting that oxidation occurred at the chlorophenyldimethyl-cyclohexenyl moiety. M3 was assigned as a hydroxylated metabolite of venetoclax with hydroxylation occurring at 3 position of cyclohexenyl ring. The structure of M3 was further confirmed by comparing MS/MS fragmentation pattern and chromatographic retention time with the reference standard.

M4. M4 was detected in plasma and feces with a protonated molecular ion of *m/z* 884.3220. Measured accurate mass data suggested the molecular formula of $C_{45}H_{51}ClN_7O_8S^+$. Collision-induced dissociation of M4 generated fragment ions at 636.2229 and 321.1343, suggesting that oxidation occurred at the chlorophenyldimethyl-cyclohexenyl moiety. The M4 structure was tentatively assigned as a hydroxylated metabolite of venetoclax.

M7. M7 was observed in feces with a protonated molecular ion at *m/z* 842.3096. Measured accurate mass data suggested the molecular formula of $C_{43}H_{49}ClN_7O_7S^+$. Collision-induced dissociation of M7 generated a fragment ion at *m/z* 610.2073. M7 was tentatively assigned as a metabolite with the loss of C_2H_2 from the piperazine ring of parent drug.

M10. M10 was detected in plasma and feces with a protonated molecular ion at *m/z* 898.3007. Measured accurate mass data suggested the molecular formula of $C_{45}H_{49}ClN_7O_9S^+$. Collision-induced dissociation of M10 generated a fragment ion at *m/z* 666.2003, suggesting that modification occurred at the pyrolopyridinyloxy tetrahydropyranylmethylamino nitrophenylsulfonyl piperazinal benzamide moiety. M10 was tentatively assigned as a dihydroxylation and dehydrogenation metabolite of parent drug.

M19. M19 was detected in feces with a protonated molecular ion at *m/z* 916.3106. Measured accurate mass suggested the molecular formula of $C_{45}H_{51}ClN_7O_{10}S^+$. Collision-induced dissociation of M19 showed fragment ions at *m/z* 898.3000 (loss of water), *m/z* 668.2128 and *m/z*

321.1343, Suggesting that oxidation occurred at the chlorophenyltrimethylcyclohexenyl moiety and the dioxidation occurred at the tetrahydropyranylmethylaminonitrophenylsulfonylamide moiety. M19 was proposed to be formed from tri-hydroxylation of parent drug.

M22. M22 was detected in feces with a protonated molecular ion at *m/z* 900.3173. Measured accurate mass suggested the molecular formula of $C_{45}H_{51}ClN_7O_9S^+$. Collision-induced dissociation of M22 showed the fragment ion at *m/z* 882.3047, resulting from loss of H_2O. M22 was proposed to be formed from di-hydroxylation of parent drug.

M24. M24 was detected in feces with a protonated molecular ion at *m/z* 900.3159, suggesting a molecular formula of $C_{45}H_{51}ClN_7O_9S^+$. Collision-induced dissociation of M24 showed fragment ions at *m/z* 882.3050 and *m/z* 864.2951, resulting from the loss of H_2O. M24 was proposed to be the di-hydroxylated metabolite of parent drug.

M25. M25 was detected in feces with a protonated molecular ion at *m/z* 900.3158, suggesting a molecular formula of $C_{45}H_{51}ClN_7O_9S^+$. Collision-induced dissociation of M25 showed the fragment ion at *m/z* 882.3047, resulting from the loss of H_2O. M25 was proposed to be formed from di-hydroxylation of parent drug.

M38. M38 was detected in feces with a protonated molecular ion at *m/z* 900.3179, suggesting a molecular formula of $C_{45}H_{51}ClN_7O_9S^+$. Collision-induced dissociation of M38 showed fragment ions at *m/z* 882.3025 (loss of water), *m/z* 668.2057 and 321.1333, suggesting that modification occurred at the tetrahydropyranylmethylaminonitrophenylsulfonylamide moiety. M38 was proposed to be a di-hydroxylation metabolite of parent drug.

M39. M39 was detected in feces with a protonated molecular ion at *m/z* 916.3063. Measured accurate mass suggested a molecular formula of $C_{45}H_{51}ClN_7O_{10}S^+$. Collision-induced dissociation

of M39 showed fragment ion at *m/z* 898.2992 (loss of water). M39 was proposed to be a tri-hydroxylation metabolite of parent drug.

M40. M40 was detected in feces with a protonated molecular ion at *m/z* 916.3115. Measured accurate mass suggested a molecular formula of $C_{45}H_{51}ClN_7O_{10}S^+$. Collision-induced dissociation of M40 showed fragment ions at *m/z* 668.2129 and *m/z* 321.1344, suggesting oxidation occurred at the chlorophenyltrimethylcyclohexenyl moiety and di-oxidation occurred at the tetrahydropyranylmethylamino-nitrophenylsulfonylamide moiety. M40 was proposed to be a tri-hydroxylation metabolite of parent drug.

M41. M41 was detected in feces with a protonated molecular ion at *m/z* 916.3131. Measured accurate mass suggested a molecular formula of $C_{45}H_{51}ClN_7O_{10}$. Collision-induced dissociation of M41 showed fragment ion at *m/z* 668.2119, which suggested that oxidation occurred at the chlorophenyltrimethylcyclohexenyl moiety and di-oxidation occurred at the pyrolopyridinyloxy tetrahydropyranylmethylaminonitrophenylsulfonyl piperazinal benzamide moiety. M41 was proposed be a tri-hydroxylation metabolite of parent drug.

M42. M42 was detected in feces with a protonated molecular ion at *m/z* 916.3123. Measured accurate mass suggested a molecular formula of $C_{45}H_{51}ClN_7O_{10}S^+$. Collision-induced dissociation of M42 showed fragment ion at *m/z* 668.2110, which suggested that oxidation occurred at the chlorophenyltrimethylcyclohexenyl moiety and di-oxidation occurred at the pyrolopyridinyloxy tetrahydropyranylmethylaminonitrophenylsulfonyl piperazinal benzamide moiety. M43 was proposed be a tri-hydroxylation metabolite of parent drug.

M43. M43 was detected in feces with a protonated molecular ion at *m/z* 870.3414, suggesting a molecular formula of $C_{45}H_{53}ClN_7O_7S^+$. Collision-induced dissociation of M43 showed the key fragment ions at *m/z* 852.3307 (loss of water), *m/z* 638.2371 and *m/z* 553.2358, suggesting that the

di-oxidation occurred at the tetrahydropyranylmethylaminoaniline sulfonylamide moiety, followed by reduction of the nitrophenyl moiety. M43 was proposed be a di-hydroxylation and nitro reduction metabolite of parent drug.

M44. M44 was detected in feces with a protonated molecular ion at *m/z* 570.2632, suggesting a molecular formula of $C_{33}H_{37}ClN_5O_2^+$, a loss of 298 amu from the parent drug resulting from the cleavage of the sulfonamide bond. Collision-induced dissociation of M44 showed the key fragment ions at *m/z* 338.1611 (loss of chlorophenyltrimethylcyclohexenyl moiety) and *m/z* 321.1343. M44 was proposed to be a benzamide metabolite by the cleavage of sulfonamide.

M45. M45 was detected in feces with a protonated molecular ion at *m/z* 868.3255, suggesting a molecular formula of $C_{45}H_{51}ClN_7O_7S^+$. Collision-induced dissociation of M45 showed the key fragment ions at *m/z* 606.2484, *m/z* 583.2104 and *m/z* 321.1345, which suggested that the di-oxidation and dehydrogenation occurred at the chlorophenyltrimethylcyclohexenyl moiety. M45 was proposed be a di-hydroxylation, dehydrogenation, and nitro reduction metabolite of parent drug.

Supplemental Table 2.

Species: Dose	Compound	C_{max} (µg/mL)	AUC_{0-24} (µg•hr/mL)	Exposure Multiples[a]
Mouse 600 mg/kg/day	M27	0.062	0.76	0.05x
Dog 100 mg/kg/day	M27	0.085	1.27	0.09x
Human 400 mg/day	M27	0.686	14.1	

[a] Exposure multiples were estimated by dividing steady state exposures in mouse or dog by human steady state exposures at 400 mg dose. N=3 in each species.